IEEE Systems Journal (Volume: 13 , Issue: 3 , Sept. 2019)

Optimal Precoder Designs for Sum-Utility Maximization in SWIPT-Enabled Multi-User MIMO Cognitive Radio Networks

Changick Song, *Member, IEEE*, Hoon Lee, *Member, IEEE*, and Kyoung-Jae Lee, *Member, IEEE*

***Abstract*—In this paper, we study a generalized framework that combines the three major techniques for 5G communication systems such as the multi-user multi-input multi-output (MuMIMO) techniques for spectral efficiency enhancement, the cognitive radio (CR) techniques for spectrum sharing, and the simultaneous wireless information and power transfer (SWIPT) techniques for convenient power supplies, which is called a MuMIMO-CR-SWIPT network. In this system, we have one base-station that simultaneously supports multiple information decoding (ID) and energy harvesting users under a condition that interference power to the primary ID (P-ID) receivers stays below a certain threshold. With this scenario, our goal is to design an optimal precoder that maximizes the sum-utility cost function for the ID users while satisfying the transmit power constraint at the BS, the energy requirement at each EH user, and the interference power constraint at each P-ID user. As we consider a general sum-utility cost function that puts together different target utilities in a general MuMIMO-CR-SWIPT environment, the previous works for each of the MuMIMO, CR, and SWIPT systems are casted as particular solutions of our framework. The problem has been considered to be challenging, since the weighted minimum mean-squared error problem transformation no longer resolves the non-convexity of the original problem. In this paper, we settle such an issue by demonstrating that the WMMSE transformation guarantees zero-duality gap between the primal and dual problems. Based on the observation, we attain the optimal precoder by solving the dual problem through the sub-gradient ellipsoid method. We also propose a simplified algorithm for the case of a single ID user, which is shown to achieve the globally optimum. Finally, we demonstrate the optimality and efficiency of the proposed algorithms through numerical simulation results.**

***Index Terms*—Cognitive radio (CR), multiuser (MIMO), SWIPT, sum utility maximization, weighted MMSE.**

Manuscript received April 13, 2018; revised August 21, 2018; accepted October 6, 2018. This work was supported by the National Research Foundation of Korea through the Korea Government (MSIT) under Grant NRF-2018R1D1A1B07049824. The work of K.-J. Lee was supported by the Institute for Information and Communications Technology Promotion Grant funded by the Korea Government (MSIT) (2018-0-00812. *(Corresponding author: Kyoung-Jae Lee.)*

C. Song is with the Department of Electronic Engineering, Korea National University of Transportation, Chungju 27469, South Korea (e-mail: c.song@ut.ac.kr).

H. Lee is with the Information Systems Technology and Design Pillar, Singapore University of Technology and Design, Singapore 487372 (e-mail: hoon_lee@sutd.edu.sg).

K.-J. Lee is with the Department of Electronics and Control Engineering, Hanbat National University, Daejeon 34158, South Korea (e-mail: kyoungjae@hanbat.ac.kr).

Digital Object Identifier 10.1109/JSYST.2018.2875762

I. Introduction

RECENTLY, cognitive radio (CR) technologies have been developed as a promising solution for efficient spectrum usage. It was shown that even when the licensed primary users are active for transmission or reception, the unlicensed secondary users are still able to share the spectrum opportunistically with the active primary users by utilizing multiple transmit antennas and properly designing its transmit spatial spectrum. The fundamental limit of such a network was studied in [1]. More feasible approaches have also been discussed in [2]–[4] and references therein to provide linear precoders that maximize the weighted sum-rate (WSE) or minimize the minimum mean-squared error (MMSE) of the secondary users by imposing constraints on the interference power at the primary receivers.

In the meantime, the idea of energy harvesting (EH) has recently been introduced to provide convenient and sustainable energy supplies. In particular, considering the information carrying radio frequency (RF) signals as a new energy source for the EH, simultaneous wireless information and power transfer (SWIPT) techniques have garnered a lot of interest. Recently, new advances in hardware technologies have enabled power to be transferred and harvested efficiently over a distance [5], [6]. However, appropriate precoder designs based on multi-input multi-output (MIMO) antennas are still essential to fully exploit the advantages of the SWIPT by concurrently maximizing the spectral efficiency for the information decoding (ID) users and the amount of harvested energy for the EH users. From this viewpoint, various precoding techniques have been investigated in multi-user SWIPT environments [7]–[17].

Zhang and Ho [7] considered a two-user broadcasting channel (a single ID and a single EH) in terms of maximizing the information rate to the ID user under a single EH constraint. The result was then re-interpreted in [8]–[10] with respect to the weighted MMSE (WMMSE) criterion, and more generalized and efficient solutions were provided. Xu *et al.* [11] solved a transmit power minimization problem under multiple signal-to-noise ratio (SNR) and EH constraints for the ID and EH users, respectively. However, all the users were restricted to having a single antenna. To take into account the general multi-user MIMO (MuMIMO) SWIPT environment where all ID and EH users are equipped with multiple antennas, Rubio *et al.* [12] proposed a precoder design based on the multi-objective cost function to overcome the non-convex problem of the transmit covariance matrices in multi-stream MuMIMO SWIPT networks. However, high computational complexity is still an issue, because a string of semi-definite programming (SDP) problems should be solved for each filter update during the iterative algo-

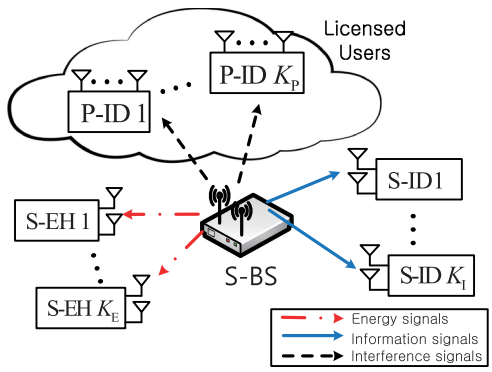

Fig. 1. Schematic diagram for the proposed MuMIMO-CR-SWIPT networks.

rithm. In [13]–[15], the security issue has been addressed for the beamforming designs in the multi-antenna SWIPT networks.

In the SWIPT networks, it is often required to achieve the high received signal power to satisfy the energy requirement of each EH user, which may also incur strong interference to other nearby users and networks that utilize the same spectrum. Therefore, a practical SWIPT system should come with a proper interference management technique. To address such an issue, an efficient beamforming scheme has been developed in [18] to control the interference power to the primary networks in the CR-SWIPT topology. However, the study was limited to a single antenna environment with a single ID user.

In this paper, we investigate the optimal precoder designs in a general *MuMIMO-CR-SWIPT* network, where one secondary base-station (S-BS) supports multiple secondary ID (S-ID) and multiple secondary EH (S-EH) users all having multiple antennas by utilizing the licensed spectrum assigned to the primary ID (P-ID) users as shown in Fig. 1. We model our transmitter design as a unified framework for sum-utility maximization in the MuMIMO-CR-SWIPT systems, in which the previous studies in [7], [8], [9], [11], [12], and [18] are shown to be particular solutions of the proposed framework. The sum-utility maximization problem has initially been proposed in [19] to address different types of cost functions, such as the WSR, proportional fairness (PF), and harmonic mean rate (HMR) at once in the conventional MuMIMO systems. However, it remains unclear whether such existing solutions are applicable to the general MuMIMO-CR-SWIPT networks, because the WMMSE transformation techniques in [19] no longer resolve the non-convexity of the original problem.

A main difference point of our study from the aforementioned previous works is that we treat a general sum-utility maximization problem in general MuMIMO-CR-SWIPT systems, where the transmit power constraint at the S-BS, the interference power constraint at each P-ID user, and the EH constraint at each EH-user are simultaneously satisfied. Although the previous work in [18] also considers the CR-SWIPT topology, it is confined to the single receive antenna scenarios with a single S-ID user, which results in an easy-to-solve convex problem. In contrast, our problem is generally non-convex, and thus more challenging to solve. Note that the conventional SDP approach as in [12] is not directly applicable to our problem due to the non-linear utility cost functions.

The contribution of the paper is summarized as follows.

1) In Section III, first, we propose an optimal energy transmission scheme to maximize the amount of energy harvested at the S-EH users under the CR constraints. We show that the rank-1 transmission is optimal for maximizing the weighted sum of harvested energy regardless of the number of EH and CR constraints. Then, we develop an efficient algorithm to find the optimal energy beam vector based on the subgradient ellipsoid method. This scheme enables us to identify a feasible range of the energy thresholds for the subsequent precoder designs.
2) In Section IV, we propose an optimal precoder design for general sum-utility maximization in the MuMIMO-CR-SWIPT networks. First, we mathematically demonstrate that the WMMSE problem transformation gives rise to a strong duality between the primal and its dual problems in terms of the precoding matrix. Based on the observation, we propose an efficient algorithm to find an optimal precoder by adopting the ellipsoid and alternating optimization methods in its inner and outer iterations, respectively. The proposed algorithm converges at least to a locally optimal point, and thus can be made arbitrarily close to the global optimum with the aid of multiple initial points. A modified algorithm is also introduced to address the zero-interference constraints to the primary users.
3) In Section V, we provide a simplified algorithm that achieves a globally optimal solution considering a special case of the S-BS supporting one S-ID user at a time in a time division multiple access (TDMA) manner, which is called *single user MIMO (SuMIMO) CR SWIPT*. Unfortunately, the problem is still non-convex. To resolve the problem, we first determine an optimal precoder structure through the Lagrange dual analysis. Then, we propose an efficient algorithm to find the remaining dual variables based on the subgradient ellipsoid method. We show that the proposed solution finds a globally optimal point without the aid of the alternating optimization and the multiple initial points, and thus is efficient. The resulting solution is also exploited as a useful outerbound of the MuMIMO-CR-SWIPT system by presuming that the multiple S-ID users act like a single macro user with ideal multiuser cooperation.
4) In Section VI, we provide an in-depth discussion on the proposed designs from the practical implementation perspectives, such as the required channel state information (CSI) at each node, the channel estimation procedure, and the computational complexity.
5) Finally, in Section VII, we offer extensive simulation results to demonstrate the efficiency of the proposed designs. We first confirm that the proposed SuMIMO design attains the global optimum. Then, we verify the optimality of the MuMIMO design by observing that the performance approaches its SuMIMO outerbound with the aid of multiple initial points. One interesting observation is that the optimal point is achievable with only a few initial points in the low-to-medium SNR region, although a larger number of initial points may be still needed as SNR grows high. Obviously, the proposed MuMIMO design based on the WSR utility achieves the best WSR performance. However, the PF and HMR designs may be preferred over the WSR design in terms of the rate balancing among the S-ID users.

Notations: Throughout the paper, boldface upper and lowercase letters denote matrices and vectors, respectively. The superscripts $(\cdot)^{\mathsf{T}}$ and $(\cdot)^{\mathsf{H}}$ stand for the transpose and

Hermitian-transpose operations, respectively. We use $\mathsf{E}[\cdot]$, $\det(\cdot)$, and $\mathsf{Tr}(\cdot)$ to denote the expectation, determinant, and trace operations, respectively. A notation $\text{blkdiag}\{\mathbf{A}_1, \ldots, \mathbf{A}_K\}$ represents a blockwise diagonal matrix with matrices $\mathbf{A}_1, \ldots, \mathbf{A}_K$. For a matrix $\mathbf{A}$, we define $\delta_{\max}(\mathbf{A})$, $\delta_{\min}(\mathbf{A})$, $(\mathbf{A})_+$, and $\nabla f(\mathbf{A})$ as the largest eigenvalue, the smallest eigenvalue, the element-wise $\max(\cdot, 0)$ operation, and the gradient of $f(\cdot)$ at $\mathbf{A}$, respectively. Also, we define $\left[\{\mathbf{A}_i\}_{i=1}^K\right] = [\mathbf{A}_1, \ldots, \mathbf{A}_K]$ as a matrix consisting of $\mathbf{A}_i$'s from $i = 1$ to K. We define $\mathbf{I}_N$ as an $N \times N$ identity matrix.

II. System Model

As shown in Fig. 1, we consider a general MuMIMO-CR-SWIPT network where an unlicensed S-BS with M antennas supports K_I S-ID users and K_E S-EH users by sharing the licensed spectrum assigned to the K_P P-ID users such that the performance degradation of each active primary link is within a tolerable margin. It is generally assumed that each of the S-ID, S-EH, and P-ID users has N_I, N_E, and N_P number of antennas, respectively. Here, we assume that M is sufficiently large such that $M > K_P N_P$ to circumvent a feasibility issue for the zero-interference conditions as will be described in more detail in Section IV-C.

Define $\mathbf{x} = [\mathbf{x}_1^\mathsf{T}, \ldots, \mathbf{x}_{K_I}^\mathsf{T}]^\mathsf{T} \sim \mathcal{CN}(0, \mathbf{I}_{K_I N_I})$ and $\mathbf{n} = [\mathbf{n}_1^\mathsf{T}, \ldots, \mathbf{n}_{K_I}^\mathsf{T}]^\mathsf{T} \sim \mathcal{CN}(0, \sigma_n^2 \mathbf{I}_{K_I N_I})$ as the baseband signal vectors for the data and noise associated with the S-ID users, respectively. Then, considering the narrow-band flat fading channels, the received signal vector $\mathbf{y} = [\mathbf{y}_1^\mathsf{T}, \ldots, \mathbf{y}_{K_I}^\mathsf{T}]^\mathsf{T} \in \mathbb{C}^{K_I N_I}$ for K_I S-ID users can be expressed as

$$\mathbf{y} = \mathbf{H}\mathbf{F}\mathbf{x} + \mathbf{n} \tag{1}$$

where $\mathbf{H} \in \mathbb{C}^{K_I N_I \times M}$ and $\mathbf{F} \in \mathbb{C}^{M \times K_I N_I}$ denote the channel and the precoding matrices from the S-BS to the S-ID users, respectively. Specifically, we have

$$\mathbf{H} = \left[\{\mathbf{H}_k^\mathsf{T}\}_{k=1}^{K_I}\right]^\mathsf{T} \quad \text{and} \quad \mathbf{F} = \left[\{\mathbf{F}_k\}_{k=1}^{K_I}\right]$$

where $\mathbf{H}_k \in \mathbb{C}^{N_I \times M}$ and $\mathbf{F}_k \in \mathbb{C}^{M \times N_I}$ represent the channel and precoding matrices from the S-BS to the kth S-ID user, respectively. Thus, the received signal at the kth S-ID $\mathbf{y}_k$ can be rephrased by

$$\mathbf{y}_k = \mathbf{H}_k \mathbf{F}_k \mathbf{x}_k + \sum_{m=1, m \neq k}^{K_I} \mathbf{H}_k \mathbf{F}_m \mathbf{x}_m + \mathbf{n}_k,$$

which leads to the information rate R_k to the kth S-ID user as

$$R_k = \log\det\left(\mathbf{F}_k^\mathsf{H} \mathbf{H}_k^\mathsf{H} \mathbf{R}_{n,k}^{-1} \mathbf{H}_k \mathbf{F}_k + \mathbf{I}_{N_I}\right) \tag{2}$$

where $\mathbf{R}_{n,k} \triangleq \sum_{m \neq k} \mathbf{H}_k \mathbf{F}_m \mathbf{F}_m^\mathsf{H} \mathbf{H}_k^\mathsf{H} + \sigma_n^2 \mathbf{I}_{N_I}$ denotes the effective noise covariance matrix. For simplicity, here, we ignored the interference from the primary transmitter to the S-ID users, but the result can be applied to more general cases. For notational convenience, we also define a stacked noise covariance as $\mathbf{R}_n \triangleq \text{blkdiag}[\mathbf{R}_{n,1}, \ldots, \mathbf{R}_{n,K_I}]$.

Define the downlink channel matrices from the S-BS to the ith S-EH and the jth P-ID users as $\mathbf{G}_i \in \mathbb{C}^{N_E \times M}$ and $\mathbf{T}_j \in \mathbb{C}^{N_P \times M}$, respectively. Then, by employing the conventional linear EH model in [7], the amount of energy that can be harvested per unit time at the ith EH-user is quantified as $\rho \|\mathbf{G}_i \mathbf{F}\|_F^2 = \rho \mathsf{Tr}(\mathbf{F}^\mathsf{H} \mathbf{G}_i^\mathsf{H} \mathbf{G}_i \mathbf{F})$ where $0 < \rho < 1$ represents the RF-to-energy conversion efficiency. For ease of presentation, we set $\rho = 1$ unless stated otherwise. Similarly, one can define the total interference power at the jth P-ID user as $\|\mathbf{T}_j \mathbf{F}\|_F^2 = \mathsf{Tr}(\mathbf{F}^\mathsf{H} \mathbf{T}_j^\mathsf{H} \mathbf{T}_j \mathbf{F})$ [4].

We consider the quasi-static fading environment, where the channel matrices are approximately constant over a few transmission blocks. Then, considering the time division duplex (TDD) scheme, the S-BS obtains the CSI of all links utilizing the uplink reference signals from the users, while each S-ID user obtains its own CSI by leveraging the downlink training from the S-BS. Then, we can formulate a precoder design problem for sum-utility maximization in the MuMIMO-CR-SWIPT networks as

$$\begin{aligned}
\text{(P-1)} \quad & \max_{\mathbf{F}} \sum_{k=1}^{K_I} U_k(R_k) \\
\text{s.t.} \quad & C_{\text{BS}} : \mathsf{Tr}\left(\mathbf{F}^\mathsf{H}\mathbf{F}\right) \leq P_T \\
& C_{\text{EH}} : \mathsf{Tr}\left(\mathbf{F}^\mathsf{H} \mathbf{G}_i^\mathsf{H} \mathbf{G}_i \mathbf{F}\right) \geq E_{\text{th},i} \text{ for } i = 1, \ldots, K_E \\
& C_{\text{CR}} : \mathsf{Tr}\left(\mathbf{F}^\mathsf{H} \mathbf{T}_j^\mathsf{H} \mathbf{T}_j \mathbf{F}\right) \leq I_{\text{th},j} \text{ for } j = 1, \ldots, K_P
\end{aligned}$$

where C_{BS} denotes the transmit power constraint at the S-BS and C_{EH} and C_{CR} represent individual harvested energy and interference constraints for the S-EH and P-ID users, respectively. Here, $E_{\text{th},i}$ and $I_{\text{th},j}$ refer to the target energy level at the ith S-EH user and the target interference level at the jth P-ID user, respectively. $U_k(\cdot)$ indicates a utility function that is for example given by $U_k(R_k) = \alpha_k R_k$, $U_k(R_k) = \log R_k$, and $U_k(R_k) = -R_k^{-1}$ for the WSR, PF, and HMR, respectively. Note that (P-1) is generally non-convex, and thus is difficult to solve in its current form. Throughout the paper, we assume that the S-BS solves (P-1) with global perfect CSIs of $\{\mathbf{H}_k, \mathbf{G}_i, \mathbf{T}_j \quad \forall k, i, j\}$. More details about the required CSIs at each node and the corresponding channel acquisition procedure will be discussed later in Section VI.

III. Achievable Energy Region

When the EH requirements at the S-EH users grow too high, the system may become infeasible due to limited transmit power at the S-BS. Therefore, it is important to check whether the system is feasible or not before solving the problem in (P-1). In this section, we formulate an weighted sum harvested energy maximization problem in the CR-SWIPT topology to identify the Pareto optimal boundary points of the achievable energy region in (P-1) and provide an efficient algorithm to find a solution.

Let us set $w_i \geq 0$ as an weight factor for the harvested energy at the ith EH user such that $\sum_{i=1}^{K_E} w_i = 1$. Then, the weighted sum harvested energy maximization problem can be formulated as

$$\begin{aligned}
\text{(P-2)} \quad & \min_{\mathbf{S} \succeq \mathbf{0}} -\sum_{i=1}^{K_E} w_i \mathsf{Tr}\left(\mathbf{G}_i \mathbf{S} \mathbf{G}_i^\mathsf{H}\right) \\
\text{s.t.} \quad & \mathsf{Tr}\left(\mathbf{S}\right) \leq P_T \\
& \mathsf{Tr}\left(\mathbf{T}_j \mathbf{S} \mathbf{T}_j^\mathsf{H}\right) \leq I_{\text{th},j} \quad \forall j.
\end{aligned}$$

The above problem is convex, for which the strong duality holds. Here, we have relaxed a constraint $\mathbf{S} = \mathbf{F}\mathbf{F}^\mathsf{H}$, but one may recognize from the following proposition that a precoding matrix that is given in the form $\mathbf{F} = [\mathbf{f}\ \mathbf{0}_{M \times (K_I N_I - 1)}]$ can achieve the optimal value of (P-2). According to the weight factors w_i's, the resulting solution identifies each Pareto optimal boundary point of the achievable energy region.

TABLE I
ALGORITHM FOR SOLVING (P-3)

Initialize $\mathbf{u} \succeq \mathbf{0}$.
Repeat
Compute the subgradient of $g(\mathbf{u})$ for a given $\mathbf{u}$.
Update $\mathbf{u}$ using the ellipsoid method subject to $\mathbf{u} \succeq \mathbf{0}$.
Until $\mathbf{u}$ converges to the prescribed accuracy.
Find $\mathbf{f}$ such that $(\delta_{\max}(\mathbf{P})\mathbf{I}_M - \mathbf{P})\mathbf{f} = \mathbf{0}$ and $\|\mathbf{f}\|^2 = P_T$.

Proposition 1: With the assumption that $M > K_P N_P$, the optimum in (P-2) can be achieved by a rank-1 matrix $\mathbf{S}$ having full transmit power $\mathsf{Tr}(\mathbf{S}) = P_T$.

Proof: First, by contradiction, let us presume that the optimum of (P-2) occurs at a point where $\mathsf{Tr}(\mathbf{S}) < P_T$. Define an aggregated P-ID user channels $\mathbf{T} = [\{\mathbf{T}_j^{\mathsf{T}}\}_{j=1}^{K_P}]^{\mathsf{T}}$. Then, for $M > K_P N_P$, we can find a matrix $\mathbf{Q} \in \mathbb{C}^{M \times (M - K_P N_P)}$ to meet $\mathbf{TQ} = \mathbf{0}$. Therefore, any matrix $\mathbf{S}'$ in the form of $\mathbf{S}' = \mathbf{S} + c\mathbf{Q}\mathbf{Q}^{\mathsf{H}}$ with a constant $c > 0$ such that $\mathsf{Tr}(\mathbf{S}') = P_T$ achieves a greater amount of energy than $\mathbf{S}$ without violating all the constraints in (P-2), which contradicts to our previous presumption. Therefore, $\mathsf{Tr}(\mathbf{S}) = P_T$ is always optimal.

In the meantime, let us consider the Lagrangian as

$$\mathcal{L}_{P2} = -\sum_{i=1}^{K_E} w_i \mathsf{Tr}(\mathbf{G}_i \mathbf{S} \mathbf{G}_i^{\mathsf{H}}) + \nu(\mathsf{Tr}(\mathbf{S}) - P_T) - \mathsf{Tr}(\mathbf{\Psi S}) + \sum_{j=1}^{K_P} \mu_j \left(\mathsf{Tr}(\mathbf{T}_j \mathbf{S} \mathbf{T}_j^{\mathsf{H}}) - I_{\text{th},j}\right) \tag{3}$$

where $\nu \geq 0$, $\mu_j \geq 0$, and $\mathbf{\Psi} \in \mathbb{C}^{M \times M} \succeq \mathbf{0}$ denote the dual variables corresponding to the S-BS power constraint, the jth CR constraint, and the semi-definite constraint, i.e., $\mathbf{S} \succeq \mathbf{0}$, respectively.

Then, from the KKT conditions, we have

$$\mathbf{\Psi} = \nu \mathbf{I}_M - \mathbf{P} \succeq \mathbf{0} \text{ and } \mathbf{\Psi S} = \mathbf{0} \tag{4}$$

where $\mathbf{P} \triangleq \sum_{i=1}^{K_E} w_i \mathbf{G}_i^{\mathsf{H}} \mathbf{G}_i - \sum_j \mu_j \mathbf{T}_j^{\mathsf{H}} \mathbf{T}_j$. From the former condition in (4), we have $\nu \geq \delta_{\max}(\mathbf{P})$. However, the latter condition, i.e., $\mathbf{\Psi S} = \mathbf{0}$, only holds for $\nu = \delta_{\max}(\mathbf{P})$ because otherwise $\mathbf{\Psi}$ becomes a full-rank matrix for which there exists no $\mathbf{S} \neq \mathbf{0}$ that satisfies $\mathbf{\Psi S} = \mathbf{0}$. Therefore, we can conclude that $\nu = \delta_{\max}(\mathbf{P})$ is optimal, which implies that the optimal $\mathbf{S}$ occurs at a point where all column vectors of $\mathbf{S}$ are aligned with the eigenvector corresponding to $\delta_{\max}(\mathbf{P})$. ■

The result in Proposition 1 enables us to find a solution of (P-2) without solving the complicated SDP problem. Specifically, let us define $\mathbf{u} = \left[\{\mu_j\}_{j=1}^{K_P}\right]$. Then, by leveraging (3) and (4), we can formulate a simple dual problem of (P-2) as

$$\text{(P-3)} \quad \sup_{\mathbf{u} \succeq \mathbf{0}} \; g(\mathbf{u})$$

where $g(\mathbf{u}) \triangleq \inf_{\mathbf{S} \succeq \mathbf{0}} \mathcal{L}_{P2} = -\delta_{\max}(\mathbf{P}) P_T - \sum_{j=1}^{K_P} \mu_j I_{\text{th},j}$, which is easily solved via the subgradient ellipsoid method [21], for which it can be shown that the subgradient of $g(\mathbf{u})$ at a point $\mathbf{u}$ is given by $\{-\|\mathbf{T}_j \mathbf{p}\|^2 + I_{\text{th},j}\}_{j=1}^{K_P}$ [22]. Here, $\mathbf{p}$ denotes the eigenvector of $\mathbf{P}$ corresponding to $\delta_{\max}(\mathbf{P})$. After we find the dual optimal $\mathbf{u}$, the primary optimal precoding matrix $\mathbf{F} = [\mathbf{f} \; \mathbf{0}_{M \times (K_I N_I - 1)}]$ is computed such that $(\delta_{\max}(\mathbf{P})\mathbf{I}_M - \mathbf{P})\mathbf{f} = \mathbf{0}$ with $\|\mathbf{f}\|^2 = P_T$ from Proposition 1. The algorithm is summarized in Table I.

IV. PROPOSED MUMIMO-CR-SWIPT PRECODER DESIGNS

In this section, we provide an efficient optimization algorithm to solve the sum-utility maximization problem in (P-1) for general MuMIMO-CR-SWIPT networks.

A. WMMSE Problem Reformulation

First, we transform (P-1) to an equivalent WMMSE problem that is relatively easy to solve. Let us define $\mathbf{L}_k \in \mathbb{C}^{N_I \times N_I}$ and $\hat{\mathbf{y}}_k = \mathbf{L}_k \mathbf{y}_k$ as the linear receiver and the final observation at the kth S-ID user, respectively. Then, one can compute the MSE matrix as

$$\begin{aligned} \mathbf{C}_k &\triangleq \mathsf{E}\left[(\gamma^{-1}\hat{\mathbf{y}}_k - \mathbf{x}_k)(\gamma^{-1}\hat{\mathbf{y}}_k - \mathbf{x}_k)^H\right] \\ &= \gamma^{-2}\mathbf{L}_k\left(\mathbf{H}_k \mathbf{F}_k \mathbf{F}_k^{\mathsf{H}} \mathbf{H}_k^{\mathsf{H}} + \mathbf{R}_{n,k}\right)\mathbf{L}_k^H \\ &\quad - \gamma^{-1}\mathbf{L}_k \mathbf{H}_k \mathbf{F}_k - \gamma^{-1}\mathbf{F}_k^{\mathsf{H}} \mathbf{H}_k^{\mathsf{H}} \mathbf{L}_k^{\mathsf{H}} + \mathbf{I}_{N_I} \end{aligned} \tag{5}$$

where a new variable $\gamma > 0$ enables us to obtain an efficient algorithm.

For convenience, let us set $\mathbf{F} = \gamma \bar{\mathbf{F}}$ for unknown $\bar{\mathbf{F}}$. Then, by introducing an weight matrix $\mathbf{W}_k \in \mathbb{C}^{N_I \times N_I}$, we can reformulate (P-1) to an equivalent WMMSE problem as

$$\begin{aligned} \text{(P-4)} \quad & \inf_{\gamma, \bar{\mathbf{F}}, \{\mathbf{W}_k, \mathbf{L}_k, \forall k\}} \sum_{k=1}^{K_I} \left\{\mathsf{Tr}(\mathbf{W}_k \mathbf{C}_k) + e_k(\mathbf{W}_k)\right\} \\ \text{s.t.} \quad & \bar{C}_{\text{BS}} : \mathsf{Tr}\left(\bar{\mathbf{F}}^{\mathsf{H}} \bar{\mathbf{F}}\right) \leq \gamma^{-2} P_T, \\ & \bar{C}_{\text{EH}} : \mathsf{Tr}\left(\bar{\mathbf{F}}^{\mathsf{H}} \mathbf{G}_i^{\mathsf{H}} \mathbf{G}_i \bar{\mathbf{F}}\right) \geq \gamma^{-2} E_{\text{th},i} \quad \forall i \\ & \bar{C}_{\text{CR}} : \mathsf{Tr}\left(\bar{\mathbf{F}}^{\mathsf{H}} \mathbf{T}_j^{\mathsf{H}} \mathbf{T}_j \bar{\mathbf{F}}\right) \leq \gamma^{-2} I_{\text{th},j} \quad \forall j \end{aligned}$$

where $e_k(\mathbf{W}_k) \triangleq \eta_k(\mathbf{\Gamma}_k(\mathbf{W}_k)) - \text{Tr}(\mathbf{W}_k^{\mathsf{T}} \mathbf{\Gamma}_k(\mathbf{W}_k))$ and $\eta_k(\cdot) \triangleq -U_k(-\log\det(\cdot))$. Here, $\mathbf{\Gamma}_k(\cdot)$ denotes the inverse mapping of the gradient map $\nabla\eta_k(\cdot)$, e.g., $\nabla\eta_k(\mathbf{\Gamma}_k(\mathbf{W}_k)) = \mathbf{\Gamma}_k(\nabla\eta_k(\mathbf{W}_k)) = \mathbf{W}_k$. As long as $\eta_k(\cdot)$ is a strictly concave function for all k, the equivalence between (P-1) and (P-4) holds. Detailed proof simply follows from [19, Sec. II-B].

Although (P-4) is still jointly non-convex, it is now seen as an unconstrained convex problem with respect to each of $\mathbf{W} \triangleq \text{blkdiag}\{\mathbf{W}_1, \ldots, \mathbf{W}_{K_I}\}$ and $\mathbf{L} \triangleq \text{blkdiag}\{\mathbf{L}_1, \ldots, \mathbf{L}_{K_I}\}$ for given γ and $\bar{\mathbf{F}}$. Therefore, the optimal structures of $\mathbf{W}_k$ and $\mathbf{L}_k$ are easily acquired from the KKT zero-gradient conditions.

Let us set the Lagrangian of (P-4) as

$$\begin{aligned} \mathcal{L}_{P4} &= \mathsf{Tr}(\mathbf{WC}) + e(\mathbf{W}) + \nu\left(\mathsf{Tr}(\bar{\mathbf{F}}\bar{\mathbf{F}}^{\mathsf{H}}) - \gamma^{-2}P_T\right) \\ &\quad - \sum_{i=1}^{K_E} \lambda_i \left(\mathsf{Tr}(\bar{\mathbf{F}}^{\mathsf{H}} \mathbf{G}_i^{\mathsf{H}} \mathbf{G}_i \bar{\mathbf{F}}) - \gamma^{-2} E_{\text{th},i}\right) \\ &\quad + \sum_{j=1}^{K_P} \mu_j \left(\mathsf{Tr}(\bar{\mathbf{F}}^{\mathsf{H}} \mathbf{T}_j^{\mathsf{H}} \mathbf{T}_j \bar{\mathbf{F}}) - \gamma^{-2} I_{\text{th},j}\right) \end{aligned} \tag{6}$$

where $\nu \geq 0$, $\lambda_i \geq 0$, and $\mu_j \geq 0$ denote the dual variables corresponding to $\bar{C}_{\text{BS}}$, the ith $\bar{C}_{\text{EH}}$, and jth $\bar{C}_{\text{CR}}$ constraints, respectively. Also, here we define $e(\mathbf{W}) \triangleq \sum_{k=1}^{K_I} e_k(\mathbf{W}_k)$ and

$$\begin{aligned} \mathbf{C} &\triangleq \text{blkdiag}\{\mathbf{C}_1, \ldots, \mathbf{C}_{K_I}\} \\ &= \mathbf{L}\left(\mathbf{H}\bar{\mathbf{F}}\bar{\mathbf{F}}^{\mathsf{H}}\mathbf{H}^{\mathsf{H}} + \gamma^{-2}\sigma_n^2 \mathbf{I}_{K_I N_I}\right)\mathbf{L}^{\mathsf{H}} \\ &\quad - \mathbf{LH}\bar{\mathbf{F}} - \bar{\mathbf{F}}^{\mathsf{H}}\mathbf{H}^{\mathsf{H}}\mathbf{L}^{\mathsf{H}} + \mathbf{I}_{K_I N_I}. \end{aligned} \tag{7}$$

Then, the KKT necessary conditions for optimality are given by

$$\mathbf{L}_k\left(\mathbf{H}_k\bar{\mathbf{F}}_k\bar{\mathbf{F}}_k^{\mathsf{H}}\mathbf{H}_k^{\mathsf{H}}+\gamma^{-2}\mathbf{R}_{n,k}\right)=\bar{\mathbf{F}}_k^{\mathsf{H}}\mathbf{H}_k^{\mathsf{H}}\quad\forall k \tag{8}$$

$$\mathbf{C}_k^{\mathsf{T}}-\mathbf{\Gamma}_k(\mathbf{W}_k)=\mathbf{0}\quad\forall k \tag{9}$$

$$(\mathbf{H}^{\mathsf{H}}\mathbf{L}^{\mathsf{H}}\mathbf{W}\mathbf{L}\mathbf{H}-\sum_i\lambda_i\mathbf{G}_i^{\mathsf{H}}\mathbf{G}_i+\sum_j\mu_j\mathbf{T}_j^{\mathsf{H}}\mathbf{T}_j+\nu\mathbf{I}_M)\bar{\mathbf{F}}$$
$$=\mathbf{H}^{\mathsf{H}}\mathbf{L}^{\mathsf{H}}\mathbf{W}^{\mathsf{H}} \tag{10}$$

$$\beta+\sum_i\lambda_iE_{\text{th},i}-\sum_j\mu_jI_{\text{th},i}=\nu P_T \tag{11}$$

$$\bar{C}_{\text{BS}};\ \bar{C}_{\text{EH}};\ \bar{C}_{\text{CR}} \tag{12}$$

$$\nu\left(\mathsf{Tr}(\bar{\mathbf{F}}^{\mathsf{H}}\bar{\mathbf{F}})-\gamma^{-2}P_T\right)=0 \tag{13}$$

$$\lambda_i\left(\mathsf{Tr}(\bar{\mathbf{F}}^{\mathsf{H}}\mathbf{G}_i^{\mathsf{H}}\mathbf{G}_i\bar{\mathbf{F}})-\gamma^{-2}E_{\text{th},i}\right)=0\quad\forall i \tag{14}$$

$$\mu_j\left(\mathrm{Tr}(\bar{\mathbf{F}}^{\mathsf{H}}\mathbf{T}_j^{\mathsf{H}}\mathbf{T}_j\bar{\mathbf{F}})-\gamma^{-2}I_{\text{th},j}\right)=0\quad\forall j \tag{15}$$

where $\bar{\mathbf{F}}_k=\gamma^{-1}\mathbf{F}_k$ and $\beta=\mathrm{Tr}(\sigma_n^2\mathbf{W}\mathbf{L}\mathbf{L}^{\mathsf{H}})$. Here, the equations from (8) to (11) stem from the zero gradient conditions with respect to $\mathbf{L}_k$, $\mathbf{W}_k$, $\bar{\mathbf{F}}$, and γ, respectively, and the equations from (13) to (15) represent the complement slackness conditions. Note that (9) follows from [19, Th. 2].

By condition (8), we find the optimal receiver $\mathbf{L}_k$ as

$$\mathbf{L}_k=\bar{\mathbf{F}}_k^{\mathsf{H}}\mathbf{H}_k^{\mathsf{H}}\left(\mathbf{H}_k\bar{\mathbf{F}}_k\bar{\mathbf{F}}_k^{\mathsf{H}}\mathbf{H}_k^{\mathsf{H}}+\gamma^{-2}\mathbf{R}_{n,k}\right)^{-1}\quad\forall k \tag{16}$$

which in turn makes the MSE matrix in (5) given in a compact form of $\mathbf{C}_{L,k}=(\gamma^2\bar{\mathbf{F}}_k^{\mathsf{H}}\mathbf{H}_k^{\mathsf{H}}\mathbf{R}_{n,k}^{-1}\mathbf{H}_k\bar{\mathbf{F}}_k+\mathbf{I})^{-1}$ [23]. Then, from (9), we can update the optimal weight matrix as

$$\mathbf{W}_k=\nabla\eta_k(\mathbf{C}_{L,k}^{\mathsf{T}})\quad\forall k. \tag{17}$$

For instance, we have $\mathbf{W}_k=\alpha_k\mathbf{C}_{L,k}^{-1}$, $\mathbf{W}_k=(-(\log\det(\mathbf{C}_{L,k}))\mathbf{C}_{L,k})^{-1}$, and $\mathbf{W}_k=((\log\det(\mathbf{C}_{L,k}))^2\mathbf{C}_{L,k})^{-1}$ according to our target utilities WSR, HMR, and PF in (P-1), respectively.

B. Optimal Precoder Design

Unlike the conventional non-SWIPT designs, (P-4) is still non-convex with respect to γ and $\bar{\mathbf{F}}$, because the conflicting constraints in $\bar{C}_{\text{BS}}$, $\bar{C}_{\text{EH}}$, and $\bar{C}_{\text{CR}}$ form a non-convex feasible domain. Thus, standard CVX tools such as SeDuMi [24] are not immediately applicable even if other variables $\mathbf{W}$ and $\mathbf{L}$ are fixed. Therefore, it is most important to determine the optimal structure of γ and $\bar{\mathbf{F}}$. Once their optimal forms are identified, (P-4) is easily solved by alternately updating γ, $\bar{\mathbf{F}}$, and $\{\mathbf{W}_k,\mathbf{L}_k\quad\forall k\}$ until convergence.

First, we observe from (11) that for a fixed β, ν in (6) is expressed as a function of $\bar{\mathbf{u}}\triangleq[\lambda_1,\ldots,\lambda_{K_E},\mu_1,\ldots,\mu_{K_P}]$. Thus, we can reduce the number of unknown dual variables by 1. Also, as we have $\beta>0$, at least one variable among $\{\nu,\mu_1,\ldots,\mu_{K_P}\}$ has a non-zero positive value, which implies that at least one constraint in $\bar{C}_{\text{BS}}$ and $\bar{C}_{\text{CR}}$ must be activated due to (13) and (15). Thus, for a given $\bar{\mathbf{F}}$, we have

$$\gamma=\sqrt{\min\left(\frac{P_T}{\mathsf{Tr}(\bar{\mathbf{F}}^{\mathsf{H}}\bar{\mathbf{F}})},\left\{\frac{I_{\text{th},j}}{\mathsf{Tr}(\bar{\mathbf{F}}^{\mathsf{H}}\mathbf{T}_j^{\mathsf{H}}\mathbf{T}_j\bar{\mathbf{F}})}\right\}_{j=1}^{K_P}\right)}. \tag{18}$$

Next, we consider a Lagrange dual function of (P-4) as

$$h(\bar{\mathbf{u}})=\inf_{\gamma,\bar{\mathbf{F}}}\mathcal{L}_{P4}(\nu,\bar{\mathbf{u}},\gamma,\bar{\mathbf{F}})=\inf_{\bar{\mathbf{F}}}\bar{\mathcal{L}}_{P4}(\bar{\mathbf{u}},\bar{\mathbf{F}}) \tag{19}$$

TABLE II
ALGORITHM FOR SOLVING (P-5)

Initialize $\bar{\mathbf{u}}\succeq\mathbf{0}$.
Repeat
  Compute $\mathbf{K}$ for a given $\bar{\mathbf{u}}$.
  if $\delta_{\min}(\mathbf{K})>0$
    Compute $\bar{\mathbf{F}}^\star=\mathbf{K}^{-1}\mathbf{H}^{\mathsf{H}}\mathbf{L}^{\mathsf{H}}\mathbf{W}^{\mathsf{H}}$.
    Compute the subgradient of $h(\bar{\mathbf{u}})$.
  else
    Compute the subgradient of $\delta_{\min}(\mathbf{K})$.
  end
  Update $\bar{\mathbf{u}}$ using the ellipsoid method subject to $\bar{\mathbf{u}}\succeq\mathbf{0}$.
Until $\bar{\mathbf{u}}$ converges to the prescribed accuracy.
Set $\bar{\mathbf{F}}=\bar{\mathbf{F}}^\star$.

where $\bar{\mathcal{L}}_{P4}(\bar{\mathbf{u}},\bar{\mathbf{F}})$ is obtained by applying (11) to (6) as

$$\bar{\mathcal{L}}_{P4}=\mathsf{Tr}\big(\mathbf{W}\mathbf{L}\mathbf{H}\bar{\mathbf{F}}\bar{\mathbf{F}}^{\mathsf{H}}\mathbf{H}^{\mathsf{H}}\mathbf{L}^{\mathsf{H}}-\mathbf{W}\mathbf{L}\mathbf{H}\bar{\mathbf{F}}$$
$$-\mathbf{W}\bar{\mathbf{F}}^{\mathsf{H}}\mathbf{H}^{\mathsf{H}}\mathbf{L}^{\mathsf{H}}+\mathbf{W}\big)+e(\mathbf{W})-\sum_i\lambda_i\mathsf{Tr}(\bar{\mathbf{F}}^{\mathsf{H}}\mathbf{Z}_{E,i}\bar{\mathbf{F}})$$
$$+\sum_j\mu_j\mathsf{Tr}(\bar{\mathbf{F}}^{\mathsf{H}}\mathbf{Z}_{P,j}\bar{\mathbf{F}})+\frac{\beta\mathsf{Tr}(\bar{\mathbf{F}}^{\mathsf{H}}\bar{\mathbf{F}})}{P_T}. \tag{20}$$

Here, we define $\mathbf{Z}_{E,i}\triangleq\mathbf{G}_i^{\mathsf{H}}\mathbf{G}_i-\frac{E_{\text{th},i}}{P_T}\mathbf{I}_M$ and $\mathbf{Z}_{P,j}\triangleq\mathbf{T}_j^{\mathsf{H}}\mathbf{T}_j-\frac{I_{\text{th},j}}{P_T}\mathbf{I}_M$. Now, let us temporarily ignore the constant terms in $\bar{\mathcal{L}}_{P4}$ with respect to $\bar{\mathbf{F}}$, which makes (19) rephrased by

$$\inf_{\bar{\mathbf{F}}}\left\{\mathrm{Tr}\big(\bar{\mathbf{F}}^{\mathsf{H}}\mathbf{K}\bar{\mathbf{F}}\big)-\mathrm{Tr}\big(\mathbf{W}\mathbf{L}\mathbf{H}\bar{\mathbf{F}}\big)\right\} \tag{21}$$

where $\mathbf{K}\triangleq\mathbf{Y}-\sum_i\lambda_i\mathbf{Z}_{E,i}+\sum_j\mu_j\mathbf{Z}_{P,j}$ with $\mathbf{Y}\triangleq\mathbf{H}^{\mathsf{H}}\mathbf{L}^{\mathsf{H}}\mathbf{W}\mathbf{L}\mathbf{H}+\frac{\beta}{P_T}\mathbf{I}_M$. Now, suppose that at least one eigenvalue of $\mathbf{K}$ is non-positive with corresponding eigenvector $\mathbf{v}\in\mathbb{C}^{M\times1}$. Then, we can make (21) unbounded from below by simply setting $\mathbf{F}=[\mathbf{f}\ \mathbf{0}_{M\times(K_IN_I-1)}]$ with $\|\mathbf{f}\|^2=\infty$. Therefore, a dual feasible condition $\mathbf{K}\succ\mathbf{0}$ arises for (19), which leads us to the following dual problem as:

$$\text{(P-5)}\quad\sup_{\bar{\mathbf{u}}\succeq\mathbf{0}}\quad h(\bar{\mathbf{u}})\quad\text{s.t.}\quad\delta_{\min}(\mathbf{K})>0.$$

Proposition 2: There exists zero-duality gap between (P-4) and its dual (P-5) with respect to γ and $\bar{\mathbf{F}}$.

Proof: See Appendix A. ■

With the assistance of Proposition 2, we can find optimal $\bar{\mathbf{F}}$ through (P-5) that is solvable via the ellipsoid method for constrained problems [21], for which the subgradient of $h(\bar{\mathbf{u}})$ at a feasible point $\bar{\mathbf{u}}$ is computed by $[\{\mathsf{Tr}(\bar{\mathbf{F}}^{\star\mathsf{H}}\mathbf{Z}_{E,i}\bar{\mathbf{F}}^\star)\}_{i=1}^{K_E},\{-\mathsf{Tr}(\bar{\mathbf{F}}^{\star\mathsf{H}}\mathbf{Z}_{P,j}\bar{\mathbf{F}}^\star)\}_{j=1}^{K_P}]$. Here, $\mathbf{F}^\star$ denotes the corresponding primal optimal solution. Note that $\mathbf{K}$ is invertible for a feasible $\bar{\mathbf{u}}$ since $\delta_{\min}(\mathbf{K})>0$, and thus we have

$$\bar{\mathbf{F}}^\star=\mathbf{K}^{-1}\mathbf{H}^{\mathsf{H}}\mathbf{L}^{\mathsf{H}}\mathbf{W}^{\mathsf{H}}.$$

Otherwise if $\bar{\mathbf{u}}$ violates the dual feasible condition, i.e., $\delta_{\min}(\mathbf{K})\le0$, we compute the subgradient of $\delta_{\min}(\mathbf{K})$ as $[\{\mathbf{k}^{\mathsf{H}}\mathbf{Z}_{E,i}\mathbf{k}\}_{i=1}^{K_E},\{-\mathbf{k}^{\mathsf{H}}\mathbf{Z}_{P,j}\mathbf{k}\}_{j=1}^{K_P}]$ where $\mathbf{k}\in\mathbb{C}^{M\times1}$ represents the eigenvector of $\mathbf{K}$ corresponding to $\delta_{\min}(\mathbf{K})$. The algorithm is summarized in Table II. After finding the optimal $\bar{\mathbf{F}}$, we finally set γ as in (18), which results in the optimal precoder $\mathbf{F}=\gamma\bar{\mathbf{F}}$.

Algorithm 1 illustrates the entire WMMSE algorithm for sum-utility maximization in general MuMIMO CR SWIPT systems with K_I S-ID, K_E S-EH, and K_P P-ID users. The algorithm

converges, since each update of $\mathbf{L}$, $\mathbf{W}$, and $\mathbf{F}$ minimizes the weighted sum-MSE that is bounded from below. The converged point ensures the local optimum because all gradients with respect to $\mathbf{L}$, $\mathbf{W}$, and $\mathbf{F}$ simultaneously vanish. Nevertheless, due to jointly non-convexity of (P-4), we may need N_G different random initial points so that the resulting local minimum gets closer to the global minimum. This may require additional outer-loop iterations.

Algorithm 1: Proposed MuMIMO CR SWIPT.

Set target metric $U_k(\cdot)$.
Draw achievable energy region $(E_{\text{th},1}, \ldots, E_{\text{th},K_E})$ from Table I.
Generate N_G random initial points $\{\bar{\mathbf{F}}^{(1)}, \ldots, \bar{\mathbf{F}}^{(N_G)}\}$.
for $i_p = 1 : N_G$ **do**
  Initialize $\bar{\mathbf{F}} = \bar{\mathbf{F}}^{(i_p)}$ and compute γ from (18).
  repeat
    Compute $\mathbf{L}$ and $\mathbf{W}$ respectively from (16) and (17) for given γ and $\bar{\mathbf{F}}$.
    Find $\bar{\mathbf{F}}$ from Table II for given $\mathbf{L}$ and $\mathbf{W}$.
    Compute γ from (18) for a given $\bar{\mathbf{F}}$.
  until convergence.
  Save $\mathbf{F}^{(i_p)} = \gamma\bar{\mathbf{F}}$.
end for
Select the best one among N_G different solutions $\{\mathbf{F}^{(i_p)}\}_{i_p=1}^{N_G}$.

C. Zero-Interference Design

When $I_{\text{th},j} = 0$ for some $j \in \mathbb{K}_P$ where $\mathbb{K}_P$ denotes a subset of P-ID user indices $\{1, 2, \ldots, K_P\}$, the algorithm in Section IV may be inefficient and unstable, because we may find unnecessary dual variables that are associated with the zero-interference constraints. It is thus imperative to modify the optimization problem so that one can solve the problem more efficiently.

Define a stacked P-ID user channel matrix as

$$\mathbf{T}_{\text{stack}} = [\{\mathbf{T}_j^{\mathsf{T}}\}_{j\in\mathbb{N}}]^{\mathsf{T}} \in \mathbb{C}^{QN_I \times M} \tag{22}$$

where Q designates a cardinality of $\mathbb{N}$. As we assume that $M > QN_I$, we can also define a matrix $\mathbf{U} \in \mathbb{C}^{M\times(M-QN_I)}$ whose column vectors constitute the orthonormal basis in the null-space of $\mathbf{T}_{\text{stack}}$, i.e., $\mathbf{T}_{\text{stack}}\mathbf{U} = \mathbf{0}$ with $\mathbf{U}^{\mathsf{H}}\mathbf{U} = \mathbf{I}_{M-QN_I}$. Note that otherwise if $M \le QN_I$, the system might be infeasible.

The precoding matrix that satisfies the zero-interference constraints, i.e., $I_{\text{th},j} = 0, \forall j \in \mathbb{N}$, must be in the null-space of $\mathbf{T}_{\text{stack}}$. Therefore, without loss of optimality, the optimal precoder can be generally expressed by $\mathbf{F} = \mathbf{U}\tilde{\mathbf{F}}$ for any matrix $\tilde{\mathbf{F}} \in \mathbb{C}^{(M-QN_I)\times K_I N_I}$. Thus, applying the result to (P-1), we obtain a modified optimization problem as

$$\begin{aligned}
\text{(P-6)}\quad & \max_{\tilde{\mathbf{F}}} \sum_{k=1}^{K_I} U_k(\tilde{R}_k) \\
\text{s.t.}\quad & \mathsf{Tr}\big(\tilde{\mathbf{F}}^{\mathsf{H}}\tilde{\mathbf{F}}\big) \le P_T \\
& \mathsf{Tr}\big(\tilde{\mathbf{F}}^{\mathsf{H}}\tilde{\mathbf{G}}_i^{\mathsf{H}}\tilde{\mathbf{G}}_i\tilde{\mathbf{F}}\big) \ge E_{\text{th},i} \quad \forall i \\
& \mathsf{Tr}\big(\tilde{\mathbf{F}}^{\mathsf{H}}\tilde{\mathbf{T}}_j^{\mathsf{H}}\tilde{\mathbf{T}}_j\tilde{\mathbf{F}}\big) \le I_{\text{th},j} \quad \forall j \in \mathbb{K}_P^{\mathsf{C}}
\end{aligned}$$

where $\mathbb{K}_P^{\mathsf{C}}$ denotes a complementary set of $\mathbb{K}_P$ and $\tilde{R}_k = \log\det(\tilde{\mathbf{F}}_k^{\mathsf{H}}\tilde{\mathbf{H}}_k^{\mathsf{H}}\mathbf{R}_{n,k}^{-1}\tilde{\mathbf{H}}_k\tilde{\mathbf{F}}_k + \mathbf{I}_{N_I})$ with $\tilde{\mathbf{H}} \triangleq \mathbf{H}\mathbf{U}$, $\tilde{\mathbf{G}} \triangleq \mathbf{G}\mathbf{U}$, and $\tilde{\mathbf{T}} \triangleq \mathbf{T}\mathbf{U}$. Once we find $\tilde{\mathbf{F}}$, the resulting solution $\mathbf{F} = \mathbf{U}\tilde{\mathbf{F}}$ achieves the zero interference constraints, i.e., $I_{\text{th},j} = 0, \forall j \in \mathbb{K}_P^C$ with reduced number of dual variables by Q, and thus is efficient. The rest of derivations is the same as the previous section. Note that when we consider all zero interference, i.e., $I_{\text{th},j} = 0, \forall j$, the CR constraints in (P-6) is completely removed, which we call a *zero-forcing (ZF) design*. Further, if we have $K_E = 1$ and $U_k(\tilde{R}_k) = \tilde{R}_k$, (P-6) becomes equivalent to the one in [9].

V. Joint Optimal Solution for Single S-ID User

In practice, the S-BS may support one S-ID user at a time in a TDMA manner. In this case, our system model reduces to the SuMIMO channel with multiple CR and EH constraints, for which we can show that the WMMSE problem in (P-4) can be jointly optimized without the aid of the multiple initial points and the alternating optimization among the filters. The result in this section not only provides the globally optimal solution for the SuMIMO-CR-SWIPT system, but also serves as a theoretical performance outer bound for the MuMIMO-CR-SWIPT systems in the previous section. Throughout the section, we will drop the S-ID user index k from all variables related to the S-ID users, since we only consider $K_I = 1$. Also, the auxiliary variable γ in (5) is now included in the receiver $\mathbf{L}$ from the joint optimization perspective.

A. Joint Optimal Precoder Design

Setting $\gamma = 1$ and $\mathbf{F} = \bar{\mathbf{F}}$, and plugging (16) into (P-4), we obtain a modified WMMSE problem for $K_I = 1$ as

$$\begin{aligned}
\text{(P-7)}\quad & \inf_{\mathbf{F},\mathbf{W}} \mathsf{Tr}\big(\mathbf{W}\mathbf{C}_L\big) + e(\mathbf{W}) \\
\text{s.t.}\quad & \mathsf{Tr}\big(\mathbf{F}^{\mathsf{H}}\mathbf{F}\big) \le P_T, \\
& \mathsf{Tr}\big(\mathbf{F}^{\mathsf{H}}\mathbf{G}_i^{\mathsf{H}}\mathbf{G}_i\mathbf{F}\big) \ge E_{\text{th},i} \quad \forall i \\
& \mathsf{Tr}\big(\mathbf{F}^{\mathsf{H}}\mathbf{T}_j^{\mathsf{H}}\mathbf{T}_j\mathbf{F}\big) \le I_{\text{th},j} \quad \forall j
\end{aligned}$$

where $\mathbf{R}_n = \sigma_n^2\mathbf{I}_{N_I}$, $\mathbf{C}_L = (\mathbf{F}^{\mathsf{H}}\mathbf{H}^{\mathsf{H}}\mathbf{R}_n^{-1}\mathbf{H}\mathbf{F} + \mathbf{I}_{N_I})^{-1}$, and

$$\begin{aligned}
e(\mathbf{W}) &= \eta\big(\mathbf{\Gamma}(\mathbf{W})\big) - \mathrm{Tr}\big(\mathbf{W}^{\mathsf{T}}\mathbf{\Gamma}(\mathbf{W})\big) \\
&= -\log\det\big(\mathbf{W}\big) - N_I.
\end{aligned} \tag{23}$$

Here, (23) follows, since for $K_I = 1$ the general sum-utility maximization in (P-1) boils down to the rate maximization, i.e., $\max_{\mathbf{F}}\sum_k U_k(R_k) \Rightarrow \max_{\mathbf{F}} \log\det(\mathbf{F}^{\mathsf{H}}\mathbf{H}^{\mathsf{H}}\mathbf{R}_n^{-1}\mathbf{H}\mathbf{F} + \mathbf{I}_{N_I})$, for which the inverse mapping of $\nabla\eta(\cdot)$ is explicitly given by $\Gamma(\mathbf{W}) = (\mathbf{W}^{\mathsf{T}})^{-1}$. Note that (P-7) is still jointly non-convex, and therefore, the optimal solution is not immediate from there.

Define the Lagrangian for (P-7) as

$$\begin{aligned}
\bar{\mathcal{L}}_{P4} = {} & \mathsf{Tr}\big(\mathbf{W}(\mathbf{F}^{\mathsf{H}}\mathbf{H}^{\mathsf{H}}\mathbf{R}_n^{-1}\mathbf{H}\mathbf{F} + \mathbf{I}_{N_I})^{-1}\big) + e(\mathbf{W}) \\
& + \mathsf{Tr}\big(\mathbf{F}^{\mathsf{H}}\mathbf{M}\mathbf{F}\big) - \nu P_T + \sum_i \lambda_i E_{\text{th},i} - \sum_j \mu_j I_{\text{th},j}
\end{aligned} \tag{24}$$

with $\mathbf{M} \triangleq \nu\mathbf{I}_M - \sum_i \lambda_i\mathbf{G}_i^{\mathsf{H}}\mathbf{G}_i + \sum_j \mu_j\mathbf{T}_i^{\mathsf{H}}\mathbf{T}_i$. We first see from (24) that the optimal weight matrix for a given $\mathbf{F}$ should

be positive definite, because we have

$$\mathbf{W} = \nabla\eta(\mathbf{C}_L^{\mathsf{T}}) \tag{25}$$

$$= \mathbf{F}^{\mathsf{H}}\mathbf{H}^{\mathsf{H}}\mathbf{R}_n^{-1}\mathbf{H}\mathbf{F} + \mathbf{I}_{N_I} \tag{26}$$

where (25) follows from the optimality condition in (17). Based on the result, now we can find the optimal precoding structure $\mathbf{F}$ as described in the following proposition.

Proposition 3: The optimal solution $\mathbf{F}$ in (P-7) for a given positive definite weight matrix $\mathbf{W}$ has the form of

$$\mathbf{F}^{\star} = \mathbf{M}^{-1/2}\mathbf{V}_1\left(\mathbf{W}^{1/2}\mathbf{\Phi}_1^{-1/2} - \mathbf{\Phi}_1^{-1}\right)_+^{1/2} \tag{27}$$

where $\mathbf{V}_1 \in \mathbb{C}^{M\times N_I}$ and $\mathbf{\Phi}_1 \in \mathbb{C}^{N_I\times N_I}$ come from the following eigenvalue decomposition:

$$\mathbf{M}^{-\frac{1}{2}}\mathbf{H}^H\mathbf{R}_n^{-1}\mathbf{H}\mathbf{M}^{-\frac{1}{2}} = \mathbf{V}\mathbf{\Phi}\mathbf{V}^{\mathsf{H}} \tag{28}$$

with a unitary matrix $\mathbf{V} = [\mathbf{V}_1\ \mathbf{V}_2] \in \mathbb{C}^{M\times M}$ and a square diagonal matrix $\mathbf{\Phi} = \text{blkdiag}\{\mathbf{\Phi}_1\ \mathbf{0}\} \in \mathbb{C}^{M\times M}$ having the eigenvalues of (28) in a descending order.

Proof: See Appendix B. ■

B. Weight Matrix Design

The weight matrix $\mathbf{W}$ can be designed differently according to the applications.

1) Maximum Rate Design: Due to the equivalence between (P-1) and (P-7), the maximum rate can be achieved when both $\mathbf{F}$ and $\mathbf{W}$ jointly solve (P-7). To this end, the optimal weight matrix must satisfy the equality in (26) that is alternatively expressed by using $\mathbf{F}$ in (27) as

$$\mathbf{W} - \mathbf{I}_{N_I} = \left(\mathbf{W}^{1/2}\mathbf{\Phi}_1^{1/2} - \mathbf{I}_{N_I}\right)_+. \tag{29}$$

Thus, the kth diagonal element of $\mathbf{W}$ should become

$$w_k = \max(\phi_k, 1) \tag{30}$$

where ϕ_k denotes the kth diagonal element of $\mathbf{\Phi}_1$. It is seen from (27) that when $\phi_k < 1$ and $w_k = 1$, the kth data stream will be unused. As a result, without loss of optimality, we can set the maximum rate precoder as

$$\mathbf{F}_{\text{max-rate}} = \mathbf{M}^{-1/2}\mathbf{V}_1\left(\mathbf{I}_{N_I} - \mathbf{\Phi}_1^{-1}\right)_+^{1/2}. \tag{31}$$

2) Quality of Service (QoS) Design: For any given weight factors, the precoder in (27) minimizes the weighted sum-MSE, i.e., $\mathsf{Tr}(\mathbf{W}\mathbf{C}_L)$ in (P-7). Therefore, besides the rate maximization, the solution can be exploited for handling the error performance of each data stream so as to ensure the QoS.

Specifically, the QoS design can be achieved by setting $\mathbf{W} = \mathbf{I}_{N_I}$ and applying the unitary discrete Fourier transform (DFT) matrix $\mathbf{D} \in \mathbb{C}^{N_I\times N_I}$ to (27) as

$$\mathbf{F}_{\text{QoS}} = \mathbf{M}^{-1/2}\mathbf{V}_1\left(\mathbf{\Phi}_1^{-1/2} - \mathbf{\Phi}_1^{-1}\right)_+^{1/2}\mathbf{D}. \tag{32}$$

Here, we notify that the DFT matrix $\mathbf{D}$ enables all the MSEs, i.e., the diagonal elements of the MSE matrix $\mathbf{C}_L$ in (P-7), have the same value without changing their sum [23] [9]. Since we have $\mathbf{W} = \mathbf{I}_{N_I}$, the resulting solution minimizes the maximum MSE among data streams while maintaining the minimum sum-MSE, thereby achieving the QoS. The QoS design is particularly useful when independent messages are spatially multiplexed across the sub-channels and should be separately decoded. Note that for the case of a single S-ID user with a single antenna, i.e., $N_I = K_I = 1$, the two solutions in (31) and (32) are merged into one. Further, if $N_P = N_E = 1$, they reduce to the CR-SWIPT beamforming scheme in [15].

C. Dual Variable Optimization

The remaining problem is to determine the dual variables $\tilde{\mathbf{u}}$ in (27). Let us consider the dual problem constrained by the dual feasibility $\delta_{\min}(\mathbf{M}) > 0$ [see (33) in Appendix B] as

$$\text{(P-8)} \quad \sup_{\tilde{\mathbf{u}}} l(\tilde{\mathbf{u}}) \quad \text{s.t.} \quad \delta_{\min}(\mathbf{M}) > 0.$$

Then, following the same argument in Proposition 2, we can show that the strong duality holds between (P-7) and its dual (P-8). Therefore, the optimal dual variables in (27) can be attained by solving (P-8), which is accomplished by applying the ellipsoid method, for which the subgradient of $l(\tilde{\mathbf{u}})$ at a feasible point $\tilde{\mathbf{u}}$ is computed by $[-\mathsf{Tr}(\mathbf{F}^{\star\mathsf{H}}\mathbf{F}^{\star}) + P_T, \{\mathsf{Tr}(\mathbf{F}^{\star\mathsf{H}}\mathbf{G}_i^{\mathsf{H}}\mathbf{G}_i\mathbf{F}^{\star}) - E_{\text{th},i}\}_{i=1}^{K_E}, \{-\mathsf{Tr}(\mathbf{F}^{\star\mathsf{H}}\mathbf{T}_j^{\mathsf{H}}\mathbf{T}_j\mathbf{F}^{\star}) + I_{\text{th},i}\}_{j=1}^{K_P}]$. Otherwise if $\tilde{\mathbf{u}}$ is infeasible, i.e., $\delta_{\min}(\mathbf{M}) \le 0$, we update $\tilde{\mathbf{u}}$ utilizing the subgradient of $\delta_{\min}(\mathbf{M})$ as $[-1, \{\mathbf{m}^{\mathsf{H}}\mathbf{G}_i^{\mathsf{H}}\mathbf{G}_i\mathbf{m}\}_{i=1}^{K_E}, \{-\mathbf{m}^{\mathsf{H}}\mathbf{T}_i^{\mathsf{H}}\mathbf{T}_i\mathbf{m}\}_{j=1}^{K_P}]$, where $\mathbf{m} \in \mathbb{C}^{M\times 1}$ denotes the eigenvector of $\mathbf{M}$ corresponding to $\delta_{\min}(\mathbf{M})$. The ellipsoid updating procedure is summarized later. The algorithm finds the global optimal solution of (P-7) attributed to the strong duality of (P-7) and (P-8) as proved in Proposition 2, the primal optimal solution in Proposition 3, and the convexity of (P-8) for which the ellipsoid algorithm converges to the dual optimum [21].

VI. Discussion

In this section, we provide an in-depth discussion on the proposed precoder designs from the practical implementation perspectives.

A. Required CSIs at Each Node

In order to meet all required constraints in the CR-SWIPT networks, the S-BS must control the secondary users with global CSIs of $\{\mathbf{H}_k, \mathbf{G}_i, \mathbf{T}_j, \forall k, i, j\}$. Therefore, it is reasonable to assume that the precoding matrix $\mathbf{F}$ is computed at the S-BS. In contrast, the S-ID users do not need to compute $\mathbf{F}$, because only the information of the effective downlink channel $\mathbf{H}_k\mathbf{F}_k$ and the effective noise covariance $\mathbf{R}_{n,k}$ is sufficient for the kth S-ID user to decode its own message as shown in (2). Note that the S-EH users require neither the precoding matrix nor the CSI, since no further receive signal processing is needed for EH. There is no required CSI at the primary nodes to do with the secondary network.

B. Channel Acquisition Procedure

To achieve the potential benefits of the proposed precoder designs, an accurate channel estimation at the S-BS is essential. Thus, for channel estimation, the TDD scheme that can exploit the channel reciprocity between a transmitter and a receiver may be a better choice than the frequency division duplexing schemes. In this section, we introduce TDD-based channel acquisition procedure to achieve the required CSIs at each node.

First, in the beginning of each channel coherence block, the secondary users transmit orthogonal training sequences to the S-BS to allow the S-BS to estimate the CSIs of both $\mathbf{H}_k, \forall k$ and $\mathbf{G}_i, \forall i$. Note that the pilot transmission of the S-EH users is also achievable by using the energy stored in their own batteries or the energy that has been harvested in the previous transmission frame [25]. The S-BS also estimates the P-ID user channels $\mathbf{T}_j, \forall j$ by listening to the periodic uplink pilots transmitted from the P-ID users to the primary transmitter [2]–[4]. With the

Algorithm 2: Joint Optimal Design for $K_I = 1$.

Initialize $\tilde{\mathbf{u}} \succeq \mathbf{0}$.
repeat
  Compute $\mathbf{M}$ for a given $\tilde{\mathbf{u}}$.
  if $\delta_{\min}(\mathbf{M}) > 0$ **then**
    Set $\mathbf{W}$ and $\mathbf{D}$ as in Section V-B1 or -B2.
    Compute the primal optimal $\mathbf{F}^\star$ in (27).
    Compute the subgradient of $l(\tilde{\mathbf{u}})$.
  else
    Compute the subgradient of $\delta_{\min}(\mathbf{M})$.
  end if
  Update $\tilde{\mathbf{u}}$ using the ellipsoid method subject to $\tilde{\mathbf{u}} \succeq \mathbf{0}$.
until $\tilde{\mathbf{u}}$ converges to the prescribed accuracy.
Set $\mathbf{F} = \mathbf{F}^\star$.

TABLE III
COMPUTATIONAL COMPLEXITY

	Algorithm 1	Algorithm 2
$\mathbf{R}_n$	$\mathcal{O}(K_I^2 N_I^3 + K_I^2 N_I^2 M)$	-
γ	$\mathcal{O}(K_I N_I M^2 + K_P N_P K_I N_I M + K_P N_P K_I^2 N_I^2)$	-
$\mathbf{L}$	$\mathcal{O}(K_I N_I^3 + K_I M N_I^2)$	-
$\mathbf{W}$	$\mathcal{O}(K_I N_I^3)$	-
$\mathbf{K}$	$\mathcal{O}((K_E N_E + K_P N_P + K_I N_I) M^2 + K_I^2 N_I^2 M)$	-
$\mathbf{M}$	-	$\mathcal{O}((K_E N_E + K_P N_P) M^2)$
$\mathbf{F}^\star$	$\mathcal{O}(M^3 + K_I^3 N_I^3)$	$\mathcal{O}(M^3 + N_I M^2)$
I_{elp} [21]	$\mathcal{O}(K_E^2 + K_P^2)$	$\mathcal{O}(K_E^2 + K_P^2)$
Total	$N_G I_{\text{alt}} \{\mathcal{C}(\mathbf{R}_n, \gamma, \mathbf{L}, \mathbf{W}) + I_{\text{elp}} \mathcal{C}(\mathbf{F}^\star, \mathbf{K})\}$	$I_{\text{elp}} \mathcal{C}(\mathbf{F}^\star, \mathbf{M})$

acquired CSIs, the S-BS is now able to compute the precoding matrix $\mathbf{F}$ through Algorithms 1 or 2.

Next, during the downlink training phase, the kth S-ID can estimate the effective downlink channel $\mathbf{H}_k \mathbf{F}_k$ by utilizing the precoded training sequences at the S-BS. For example, the demodulation reference signaling in long-term evolution advanced can be employed [26]. Then, the S-BS feedforwards the effective noise covariance $\mathbf{R}_{n,k}$ to each kth S-ID user through the downlink control channels.[1]

C. Complexity Analysis

In what follows, we briefly examine the computational complexity of the proposed algorithms. As it is hard to measure the exact amount of computations, we instead calculate the order of floating point operations required to find the optimal precoder $\mathbf{F}^\star$ at the S-BS. Based on the analysis of matrix computation complexity in [22], the computational complexity of the proposed algorithms is summarized in Table III. Here, $\mathcal{C}(\{\mathcal{X}\})$ represents the required complexity for computing operation set $\{\mathcal{X}\}$, and I_{elp} and I_{alt} denote the required number of iterations for the ellipsoid and alternating optimization process, respectively.

[1]It is also possible for each S-ID user to apply the blind noise estimation scheme [27] to estimate its own effective noise.

TABLE IV
SIMULATION ENVIRONMENTS

Parameter	Value
Noise Power Spectral Density	-100 dBm/Hz
Signal Bandwidth	10 MHz
Energy Conversion Efficiency	50% ($\rho = 0.5$)
Channel Model	Rayleigh pathloss model
Pathloss Exponent	3
User Distance from S-BS	10 m
Reference Distance	1 m
Transmit Power (P_T)	$10 \sim 20$ dBm
(N_E, N_P, N_E, K_P)	$(2, 1, 2, 2)$

First, the result confirms that the SuMIMO design in Algorithm 2 indeed obtains complexity advantage over the MuMIMO design in Algorithm 1 for the case of $K_I = 1$, because the multiple initial points and the alternating optimization process are unnecessary, not to mention the additional efforts for computing the auxiliary filter matrices, i.e., $\mathcal{C}(\mathbf{R}_n, \gamma, \mathbf{L}, \mathbf{W})$. One interesting observation is that the amount of computations for Algorithms 1 and 2 increases in the orders of N_I^3 and N_I, respectively. This means that the complexity gain of Algorithm 2 will be more pronounced as the S-ID user antenna N_I grows.

However, it should be noted that as M and K_I increase, the MuMIMO design that can simultaneously support multiple S-ID users attains a significant throughput gain over the SuMIMO design based on the scheduling. Therefore, Algorithm 1 is also important for achieving high data throughput in multiuser scenarios. A careful examination on Table III reveals that the entire complexity for Algorithm 1 is mostly influenced by the number of antennas of the S-BS and the S-ID users, i.e., M and $K_I N_I$ as in the conventional non-SWIPT or non-CR MuMIMO systems [3], [9], [19]. Therefore, computational complexity of the proposed designs is comparable with those in the conventional MuMIMO systems.

VII. NUMERICAL RESULTS

In this section, we demonstrate the efficiency of the proposed algorithms for MuMIMO-CR-SWIPT networks through some numerical examples. We set the system parameters as in Table IV so that the average received signal power at each secondary user appears in a common SNR range, e.g., 10–20 dB. Throughout the section, each simulation result is based on a sample channel. As we assumed that all the S-ID, S-EH, and P-ID users are located in the same distance (10 m) from the S-BS, we can construct the channel matrices as $\mathbf{H}_k = 10^{-3/2}\mathbf{H}_k^{(w)}, \forall k$, $\mathbf{G}_i = 10^{-3/2}\mathbf{G}_i^{(w)}, \forall i$, and $\mathbf{T}_j = 10^{-3/2}\mathbf{T}_j^{(w)}, \forall j$, where the entries of $\mathbf{H}_k^{(w)}$, $\mathbf{G}_i^{(w)}$, and $\mathbf{T}_j^{(w)}$ are drawn from independent and identically distributed standard complex Gaussian based on the Rayleigh pathloss model. We consider the same noise power at all S-ID users being equal to $\sigma_n^2 = -30$ dBm and the same interference threshold for all P-ID users, i.e., $I_{\text{th},1} = I_{\text{th},2} = I_{\text{th}}$.[2]

[2]As for our simulation results, we have set the interference thresholds such that they appear between 0 and a certain positive value which is smaller than the maximum interference level that can be met by a non-CR SWIPT design, i.e., a solution with $I_{\text{th}} = \infty$. Similarly, the energy thresholds $E_{\text{th},i}, \forall i$ are also set to be in the feasible energy region, while being greater than the minimum energy levels that are automatically achievable by a non-SWIPT CR design, i.e., a solution with $E_{\text{th},i} = 0, \forall i$.

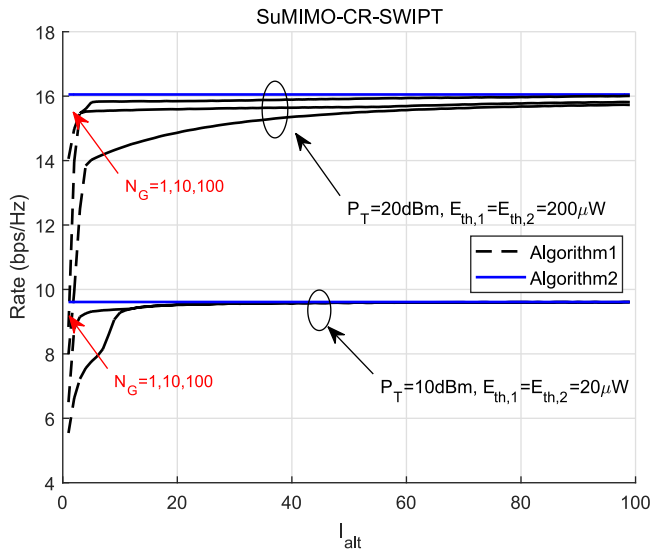

Fig. 2. Convergence trend of Algorithms 1 and 2 with $I_{\text{th}} = 0.1\,\mu$W, $K_I = 1$, and $M = N_I = 4$.

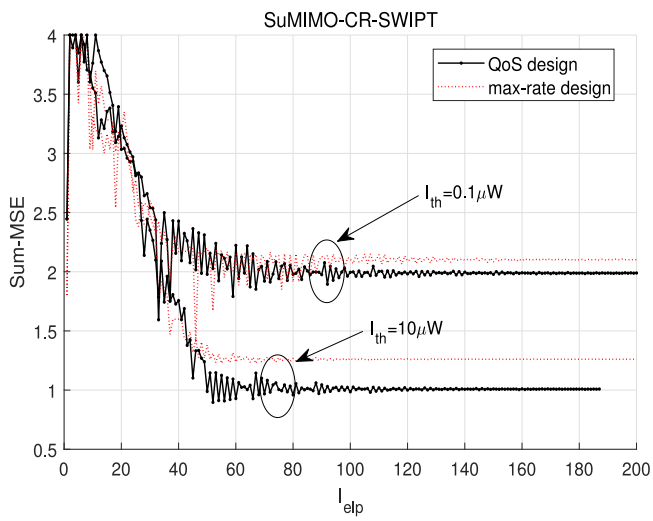

Fig. 3. Convergence trend of Algorithm 2 with $P_T = 10$ dBm, $E_{\text{th},1} = E_{\text{th},2} = 40\,\mu$W, $M = 4$, $K_I = 1$, and $N_I = 4$.

We use an initial value $\mathbf{u} = [1, 0, \ldots, 0]$ for (P-3). The initial values of (P-5) and (P-8) are similarly defined. We adopt $N_G = 100$ random initial points for Algorithm 1 unless specified otherwise. For simplicity, we set $\alpha_k = 1, \forall k$ for the WSR design.

In Figs. 2 and 3, we investigate the SuMIMO-CR-SWIPT networks with $K_I = 1$. Fig. 2 illustrates the convergence trend of Algorithms 1 and 2 for a system with $M = N_I = 4$ and $I_{\text{th}} = 0.1\,\mu$W. Interestingly, we see that a few initial points may be sufficient for Algorithm 1 in $P_T = 10$ dBm to achieve the maximum rate, while a number of initial points may be needed in $P_T = 20$ dBm. The result implies that although the WMMSE cost function in (P-4) may have a convex-like form in the low SNR region, it becomes highly non-convex as SNR goes to high. Despite the non-convexity of (P-4), we confirm that Algorithm 2 achieves the global optimum with a single initial point even without the alternating optimization process, and thus is efficient.

Fig. 3 presents the convergence trend of the ellipsoid process in Algorithm 2 in terms of the sum-MSE performance for a

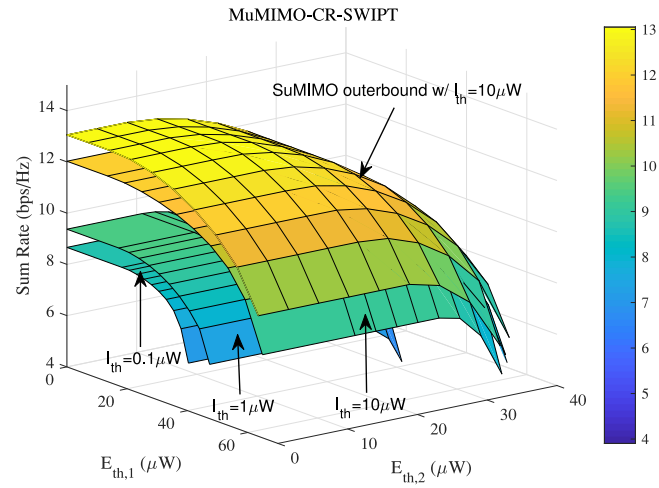

Fig. 4. Rate-energy tradeoff performance of the proposed WSR design with $P_T = 10$ dBm, $M = 4$, and $K_I = N_I = 2$.

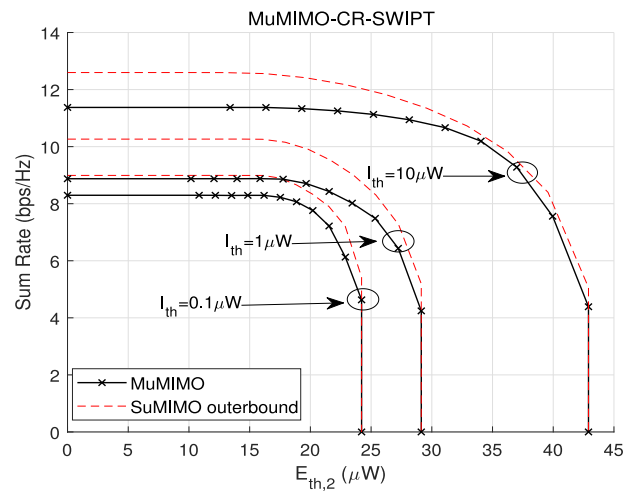

Fig. 5. Rate-energy tradeoff performance of the proposed WSR design with $P_T = 10$ dBm, $M = 4$, $K_I = N_I = 2$, and $E_{\text{th},1} = 30\,\mu$W.

system with $E_{\text{th},1} = E_{\text{th},2} = 40\,\mu$W. We observe that the QoS design in (32) achieves the minimum sum-MSE in contrast to the max-rate design. Further, the QoS design makes all sub-channels experience the same MSE. Therefore, the MSE gain of the QoS design will lead to the bit error rate performance advantage over the max-rate design [23]. Observe that the convergence speed gets slower as the interference threshold becomes tighter. The result demonstrates that when the allowed interference level at the P-ID users is very small, the zero-interference design in Section IV-C may be useful.

Figs. 4 and 5, respectively, show the rate-energy tradeoff performance in a three-dimensional (3-D) plot and in its 2-D intersection at $E_{\text{th},1} = 30\,\mu$W in an MuMIMO-CR-SWIPT system with $K_I = N_I = 2$ and $P_T = 10$ dBm. Here, we employed the WSR utility as an objective function of (P-1) to acquire the maximum sum-rate. The name of "*SuMIMO outerbound*" amounts to the case of perfect collaboration among the multiple S-ID users, which results in a single macro S-ID user with $N_I = 4$. Unlike the case of $K_I = 1$, it is generally difficult to identify whether the resulting solution is optimal or not due to the lack of knowledge on the global optimal solution. Nevertheless, we can carefully infer that the proposed solution achieves the optimum

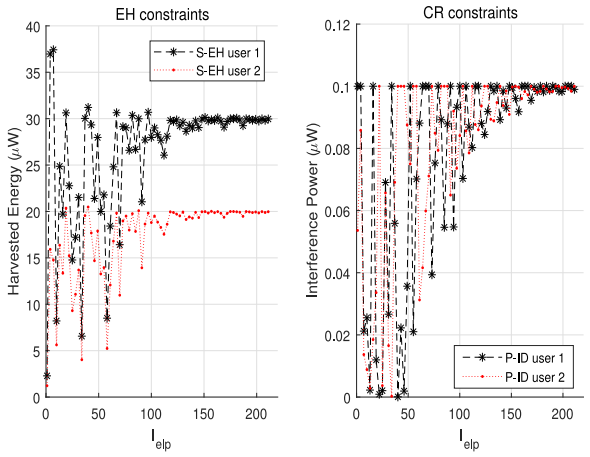

Fig. 6. Convergence trend of EH and CR constraints in MuMIMO-CR-SWIPT with $P_T = 10$ dBm, $M = 4$, $K_I = N_I = 2$, $E_{\text{th},1} = 30\,\mu$W, $E_{\text{th},2} = 20\,\mu$W, and $I_{\text{th}} = 0.1\,\mu$W.

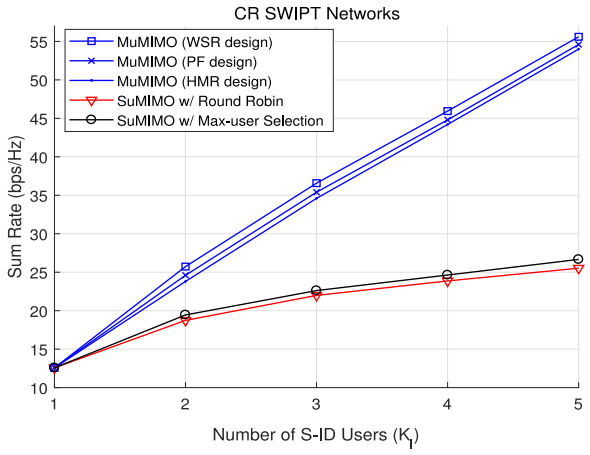

Fig. 7. WSR performance comparison with $M = K_I N_I$, $N_I = 4$, $P_T = 13$ dBm, $E_{\text{th},1} = E_{\text{th},2} = 30\,\mu$W, and $I_{th} = 0.1\,\mu$W.

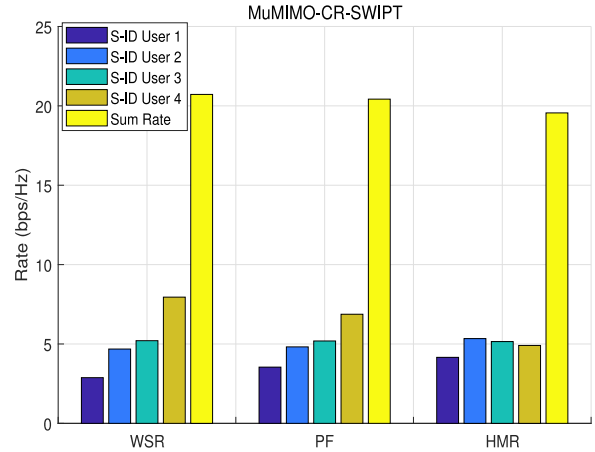

Fig. 8. Rate balancing performance of various precoder designs with $P_T = 13$ dBm, $M = 8$, $K_I = 4$, $N_I = 2$, $E_{\text{th},1} = 30\,\mu$W, $E_{\text{th},2} = 20\,\mu$W, and $I_{\text{th}} = 0.1\,\mu$W.

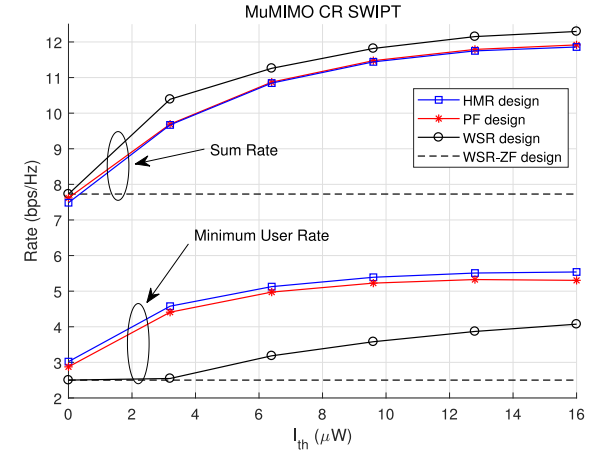

Fig. 9. WSR and minimum user rate performance of various precoder designs according to the interference thresholds I_{th} with $P_T = 10$ dBm, $M = 4$, $K_I = N_I = 2$, and $E_{\text{th},1} = E_{\text{th},2} = 10\,\mu$W.

based on the observation that all the tradeoff regions exhibit a nice convex shape and are close to their single-user outer bounds. We observe from Fig. 4 that at any information rate, there exists an unachievable energy region. This shows that the feasibility check in Section III is important before solving the problem. Obviously, as I_{th} decreases, the achievable tradeoff region will shrink to meet tighter CR constraints. One interesting observation from Fig. 5 is that as the energy threshold approaches its maximum value, the achievable rate converges to its outer-bound. This confirms our previous statement in Proposition 1 that the maximum energy of an S-EH user is achievable via a single beam vector that is pointing in one direction irrespective of the S-ID user topology.

Fig. 6 shows a snapshot of the ellipsoid process in Algorithm 1 in terms of the harvested energy and the interference power for a system with $M = 4$ and $K_I = N_I = 2$. Here, we set the threshold values as $E_{\text{th},1} = 30\,\mu$W, $E_{\text{th},2} = 20\,\mu$W and $I_{\text{th},1} = I_{\text{th},2} = 0.1\,\mu$W. The figure confirms that the proposed algorithm achieves all the required constraints. The interference power is kept below the threshold throughout the iterations attributed to the power normalizing factor γ in (18).

In Fig. 7, we plot the sum-rate performance of various precoder designs in systems with $M = N_I K_I$, $N_I = 4$, and $P_T = 13$ dBm. For a fair comparison, we introduce the round Robin scheduling or opportunistic max-user selection schemes [28] to the SuMIMO design. As expected, as K_I increases, the proposed MuMIMO designs that simultaneously support multiple S-ID users attain significant performance advantage over the SuMIMO design based on the scheduling, although the SuMIMO design attains complexity gain for the case of a single S-ID user. The gain grows larger as M and K_I increases.

In Fig. 8, we compare the rate balancing performance of various MuMIMO precoder designs for a system with $M = 8$, $K_I = 4$, $N_I = 2$, and $P_T = 13$ dBm. Obviously, the WSR design achieves the best sum-rate performance. However, the PF and HMR designs may be more attractive in terms of the worst user rate or fairness. It is observed that the HMR design yields the best balancing performance among the S-ID users at the cost of slight sum-rate performance loss.

Similar observation can be made in Fig. 9 which exhibits both the sum-rate and minimum user-rate performance for a system with $M = 4$, $K_I = N_I = 2$, and $P_T = 10$ dBm. Here, "*WSR-ZF design*" denotes the WSR solution that is obtained from (P-6) with $I_{\text{th}} = 0$ and $U_k(\tilde{R}_k) = \tilde{R}_k$. We observe that although the ZF design may provide a simpler solution, it cannot

achieve an additional performance gain from both the sum-rate and minimum user rate points of view in a situation where some amount of interference is allowable. This highlights the advantages of the interference control capability of the proposed MuMIMO-CR-SWIPT designs. As I_{th} becomes smaller, the performance variation among the different utility functions diminishes. This is because the degree of freedom of the precoder design is constrained within the null space of the P-ID user channels $\mathbf{T}$.

VIII. Conclusion

In this paper, we have investigated the optimal precoder designs for general sum-utility maximization in the MuMIMO-CR-SWIPT networks. First, we examined the optimal energy transmission scheme to identify the feasible energy region. Second, we proposed an efficient algorithm to find the optimal MuMIMO precoders by adopting the ellipsoid and alternating optimization process, for which multiple initial points may be necessary to approach the global optimum. Then, we suggested a simplified algorithm that can find a globally optimal solution without resorting to the alternating optimization as well as the multiple initial points in a special case of a single S-ID user. We also have offered an in-depth discussion on the proposed designs in terms of the computational complexity and the channel information requirement. Finally, we verified the efficiency of the proposed designs via some numerical examples. An investigation on the tradeoff between the training phase duration and channel estimation accuracy in the imperfect CSI scenarios will be an interesting topic for future works.

Appendix

A. Proof of Proposition 2

Let γ^*, $\bar{\mathbf{F}}^*$, and $\bar{\mathbf{u}}^*$ be any points that satisfy the KKT and dual feasible conditions. Define the objective function of (P-4) as $f_0(\gamma, \bar{\mathbf{F}}) = \mathsf{Tr}(\mathbf{WC}) + e(\mathbf{W})$. Then, by the weak duality theorem [24], one can show that

$$\begin{aligned} f_0(\gamma^*, \bar{\mathbf{F}}^*) &\geq h(\bar{\mathbf{u}}^*) \\ &= \inf_{\bar{\mathbf{F}}} \bar{\mathcal{L}}_{P4}(\bar{\mathbf{u}}^*, \bar{\mathbf{F}}) \\ &= \bar{\mathcal{L}}_{P4}(\bar{\mathbf{u}}^*, \bar{\mathbf{F}}^*) \\ &= f_0(\gamma^*, \bar{\mathbf{F}}^*). \end{aligned}$$

Here, the second line follows from (19) and the third line is due to the fact that $\bar{\mathcal{L}}_{P4}(\bar{\mathbf{u}}^*, \bar{\mathbf{F}})$ is convex in $\bar{\mathbf{F}}$ under the dual feasible condition $\mathbf{K} \succ \mathbf{0}$, which means that the infimum of $\bar{\mathcal{L}}_{P4}(\bar{\mathbf{u}}^*, \bar{\mathbf{F}})$ occurs at a point where its gradient vanishes, i.e., $\bar{\mathbf{F}} = \bar{\mathbf{F}}^*$. In the last line, we use the complementary slackness conditions in (13)–(15). Thus, we can conclude that $f_0(\gamma^*, \bar{\mathbf{F}}^*) = h(\bar{\mathbf{u}}^*)$.

B. Proof of Proposition 3

For any optimal $\mathbf{F}$ and an arbitrary unitary matrix $\mathbf{Q} \in \mathbb{C}^{N_I \times N_I}$, we can always find a modified solution $\hat{\mathbf{F}} = \mathbf{FQ}$ that is also optimal, since we have

$$\begin{aligned} &\log\det\left(\hat{\mathbf{F}}^{\mathsf{H}}\mathbf{H}^{\mathsf{H}}\mathbf{R}_n^{-1}\mathbf{H}\hat{\mathbf{F}} + \mathbf{I}_{N_I}\right) \\ &= \log\det\left(\mathbf{Q}^{\mathsf{H}}\mathbf{F}^{\mathsf{H}}\mathbf{H}^{\mathsf{H}}\mathbf{R}_n^{-1}\mathbf{HFQ} + \mathbf{I}_{N_I}\right) \\ &= \log\det\left(\mathbf{F}^{\mathsf{H}}\mathbf{H}^{\mathsf{H}}\mathbf{R}_n^{-1}\mathbf{HF} + \mathbf{I}_{N_I}\right). \end{aligned}$$

Here, we can choose $\mathbf{Q}$ such that $\hat{\mathbf{F}}^{\mathsf{H}}\mathbf{H}^{\mathsf{H}}\mathbf{R}_n^{-1}\mathbf{H}\hat{\mathbf{F}}$ is diagonalized without loss of optimality. In this case, the off-diagonal elements in $\mathbf{W}$ will not affect the first term of (24). In addition, by the Hadamard's inequality $\det(\mathbf{W}) \leq \prod_k w_k$, we have $e(\mathbf{W}) \geq -\sum_i \log w_k - N_I$ with $w_k > 0$ being the kth diagonal element of $\mathbf{W}$. Therefore, we see that a diagonal weight matrix $\mathbf{W}$ suffices to achieve the minimum of (24).

Next, let us define a vector of the dual variables in (24) as $\tilde{\mathbf{u}} \triangleq [\nu, \lambda_1, \ldots, \lambda_{K_E}, \mu_1, \ldots, \mu_{K_P}]$. Then, a dual feasible condition $\delta_{\min}(\mathbf{M}) > 0$ arises for $\tilde{\mathbf{u}}$, because otherwise the corresponding dual function $l(\tilde{\mathbf{u}})$ goes to $-\infty$ where

$$l(\tilde{\mathbf{u}}) \triangleq \inf_{\mathbf{F}} \bar{\mathcal{L}}_{P4}. \tag{33}$$

Under the dual feasibility, $\mathbf{M}$ is invertible, which means that one can generally express the optimal precoder as $\mathbf{F} = \mathbf{M}^{-1/2}\mathbf{V}\boldsymbol{\Sigma}$ for any matrix $\boldsymbol{\Sigma} \in \mathbb{C}^{M \times N_I}$.

Since $\mathbf{M}$ is full-rank, there are at most N_I number of non-zero eigenvalues in $\boldsymbol{\Phi}$. Let us further develop $\mathbf{F}$ as $\mathbf{F} = \mathbf{M}^{-1/2}\mathbf{V}_1\boldsymbol{\Sigma}_1 + \mathbf{M}^{-1/2}\mathbf{V}_2\boldsymbol{\Sigma}_2$ where $\boldsymbol{\Sigma}_1 \in \mathbb{C}^{N_I \times N_I}$ and $\boldsymbol{\Sigma}_2 \in \mathbb{C}^{(M-N_I)\times N_I}$ are the associated sub-matrices of $\boldsymbol{\Sigma} = [\boldsymbol{\Sigma}_1^{\mathsf{T}}\ \boldsymbol{\Sigma}_2^{\mathsf{T}}]^{\mathsf{T}}$. Then, it is true that $\mathbf{M}^{-1/2}\mathbf{V}_2\boldsymbol{\Sigma}_2 = \mathbf{0}$ since it only increases $\bar{\mathcal{L}}_{P4}$ in (24), which leads to

$$\mathbf{F} = \mathbf{M}^{-1/2}\mathbf{V}_1\boldsymbol{\Sigma}_1. \tag{34}$$

Finally, by substituting $\mathbf{F}$ in (24) with (34), we obtain a modified Lagrangian as

$$\begin{aligned} \tilde{\mathcal{L}}_{P4} = &\ \mathsf{Tr}\big(\mathbf{W}(\boldsymbol{\Sigma}_1^{\mathsf{H}}\boldsymbol{\Phi}_1\boldsymbol{\Sigma}_1 + \mathbf{I}_{N_I})^{-1}\big) + e(\mathbf{W}) + \mathsf{Tr}\big(\boldsymbol{\Sigma}_1^{\mathsf{H}}\boldsymbol{\Sigma}_1\big) \\ &- \nu P_T + \sum_i \lambda_i E_{\text{th},i} - \sum_j \mu_j I_{\text{th},j}. \end{aligned} \tag{35}$$

Now, we can verify from Lemma 1 and 2 below that the Lagrangian in (35) touches its minimal point when $\boldsymbol{\Sigma}_1$ forms a diagonal matrix because in this case $\mathbf{W}$ in (26) is given by a diagonal matrix and the first and third terms of (35) can be simultaneously minimized. Then, $\tilde{\mathcal{L}}_{P4}$ becomes convex with respect to $|\sigma_k|^2$ where σ_k denotes the kth diagonal element of $\boldsymbol{\Sigma}_1$. Thus, by setting $\frac{\partial \tilde{\mathcal{L}}_{P4}}{\partial |\sigma_k|^2} = 0$, we obtain $|\sigma_k|^2 = (w_k^{1/2}\phi_k^{-1/2} - \phi_k^{-1})_+$ with ϕ_k being the kth diagonal element of $\boldsymbol{\Phi}_1$. Finally, we have

$$\mathbf{F} = \mathbf{M}^{-1/2}\mathbf{V}_1(\mathbf{W}^{1/2}\boldsymbol{\Phi}_1^{-1/2} - \boldsymbol{\Phi}_1^{-1})_+^{1/2}.$$

Lemma 1 ([22]): For any square matrix $\mathbf{A}$, it is true that $\mathrm{Tr}(\mathbf{AA}^{\mathsf{H}}) \geq \sum_i |a_i|^2$ where a_i stands for the ith diagonal element of $\mathbf{A}$.

Lemma 2 ([29]): For any positive definite matrix $\mathbf{B}$, we have $\mathrm{Tr}(\mathbf{B}^{-1}) \geq \sum_{i=1}^{M} b_i^{-1}$ where b_i stands for the ith diagonal element of $\mathbf{B}$.

References

[1] M. Gastpar, "On capacity under receive and spatial spectrum-sharing constraints," *IEEE Trans. Inf. Theory*, vol. 53, no. 2, pp. 471–487, Feb. 2007.

[2] R. Zhang and Y. C. Liang, "Exploiting multi-antennas for opportunistic spectrum sharing in cognitive radio networks," *IEEE J. Sel. Topics Signal Process.*, vol. 2, no. 1, pp. 88–102, Feb. 2008.

[3] R. Zhang, Y. C. Liang, and S. Cui, "Dynamic resource allocation in cognitive radio networks," *IEEE Signal Process. Mag.*, vol. 27, no. 3, pp. 102–114, May 2010.

[4] K.-J. Lee and I. Lee, "MMSE based block diagonalization for cognitive radio MIMO broadcast channels," *IEEE Trans. Wireless Commun.*, vol. 10, no. 10, pp. 3139–3144, Oct. 2011.

[5] X. Lu, "Wireless networks with RF energy harvesting: A contemporary survey," *IEEE Commun. Surveys Tuts.*, vol. 17, no. 2, pp. 757–789, Apr. 2015.

[6] S. Bi, C. K. Ho, and R. Zhang, "Wireless powered communication: Opportunities and challenges," *IEEE Commun. Mag.*, pp. 117–125, Apr. 2015.

[7] R. Zhang and C. K. Ho, "MIMO broadcasting for simultaneous wireless information and power transfer," *IEEE Trans. Wireless Commun.*, vol. 12, no. 5, pp. 1989–2001, May 2013.

[8] C. Song, C. Ling, J. Park, and B. Clerckx, "MIMO broadcasting for simultaneous wireless information and power transfer: Weighted MMSE approaches," in *Proc. IEEE Global Telecommun. Conf. Workshops*, Dec. 2014, pp. 1151–1156.

[9] C. Song, J. Park, B. Clerckx, I. Lee, and K.-J. Lee, "Generalized precoder designs based on weighted MMSE criterion for energy harvesting constrained MIMO and multi-user MIMO channels," *IEEE Trans. Wireless Commun.*, vol. 15, no. 12, pp. 7941–7954, Dec. 2016.

[10] C. Song and Y. Jeon, "Weighted MMSE precoder designs for sum-utility maximization in multi-user SWIPT network-MIMO with Per-BS power constraints," *IEEE Trans. Veh. Technol.*, vol. 67, no. 3, pp. 2809–2813, Mar. 2018.

[11] J. Xu, L. Liu, and R. Zhang, "Multiuser MISO beamforming for simultaneous wireless information and power transfer," *IEEE Trans. Signal Process.*, vol. 62, no. 18, pp. 4798–4810, Aug. 2014.

[12] J. Rubio, A. P. Iserte, D. P. Palomar, and A. Goldsmith, "Joint opimization of power and data transfer in multiuser MIMO systems," *IEEE Trans. Signal Process.*, vol. 65, no. 1, pp. 212–227, Jan. 2017.

[13] Z. Zhu, Z. Chu, Z. Wang, and I. Lee, "Outage constrained robust beamforming for secure broadcasting systems with energy harvesting," *IEEE Trans. Wireless Commun.*, vol. 15, no. 11, pp. 7610–7620, Nov. 2016.

[14] Z. Zhu, Z. Chu, N. Wang, S. Huang, Z. Wang, and I. Lee, "Beamforming and power splitting designs for AN-aided secure multi-user MIMO SWIPT systems," *IEEE Trans. Inf. Forensics Security*, vol. 12, no. 12, pp. 2861–2874, Dec. 2017.

[15] Z. Zhu, Z. Chu, F. Zhou, H. Niu, Z. Wang, and I. Lee, "Secure beamforming designs for secrecy MIMO SWIPT systems," *IEEE Wireless Commun. Lett.*, vol. 7, no. 3, pp. 424–427, Jun. 2018.

[16] H. Lee, C. Song, S.-H. Choi, and I. Lee, "Outage probability analysis and power splitter designs for SWIPT relaying systems with direct link," *IEEE Commun. Lett.*, vol. 21, no. 3, pp. 648–651, Mar. 2017.

[17] Z. Zong, H. Feng, F. R. Yu, N. Zhao, T. Yang, and B. Hu, "Optimal transceiver design for SWIPT in K-user MIMO interference channels," *IEEE Trans. Wireless Commun.*, vol. 15, no. 1, pp. 430–445, Jan. 2016.

[18] F. Zhu, F. Gao, and M. Yao, "A new cognitive radio strategy for SWIPT system," in *Proc. Int. Workshop High Mobility Wireless Commun.*, 2014, pp. 73–77.

[19] Q. Shi, M. Razaviyayn, Z.-Q. Luo, and C. He, "An iteratively weighted MMSE approach to distributed sum-utility maximization for a MIMO interfering broadcast channel," *IEEE Trans. Signal Process.*, vol. 59, no. 9, pp. 4331–4340, Sep. 2011.

[20] E. Boshkovska, D. W. K. Ng, N. Zlatanov, and R. Schober, "Practical non-linear energy harvesting model and resource allocation for SWIPT systems," *IEEE Commun. Lett.*, vol. 19, no. 12, pp. 2082–2085, Dec. 2015.

[21] S. Boyd, *Ellipsoid Methods* (Notes for EE364b). Stanford, CA, USA: Stanford University, 2018.

[22] G. H. Golub and C. F. V. Loan, *Matrix Computations*. 3rd ed., Baltimore, MD, USA: The Johns Hopkins Univ. Press, 1996.

[23] D. P. Palomar, J. M. Cioffi, and M. A. Lagunas, "Joint Tx-Rx beamforming design for multicarrier MIMO channels: a unified framework for convex optimization," *IEEE Trans. Signal Process.*, vol. 51, no. 9, pp. 2381–2401, Sep. 2003.

[24] S. Boyd and L. Vandenberghe, *Convex Optimization*. Cambridge, U.K.: Cambridge Univ. Press, 2004.

[25] H. Ju, C. K. Ho, R. Zhang, and Y. L. Guan, "Throughput optimization for massive MIMO systems powered by wireless energy transfer," *IEEE J. Sel. Areas Commun.*, vol. 33, no. 8, pp. 1640–1650, Aug. 2015.

[26] E. Dahlman, S. Parkvall, J. Skold, and P. Beming, *LTE/LTE-Advanced for Mobile Broadband*. Oxford, U.K.: Elsevier, 2014.

[27] M. Frikel, W. Utschick, and J. Nossek, "Blind noise and channel estimation," in *Proc. IEEE Statist. Signal Array Process. Workshop*, Aug. 2000 pp. 141–145.

[28] A. Asadi and V. Mancuso, "A survey on opportunistic scheduling in wireless communications," *IEEE Commun. Surveys Tuts.*, vol. 15, no. 5, pp. 1671–1688, Oct.–Dec. 2013.

[29] N. Komaroff, "Bounds on eigenvalues of matrix products with an application to the algebraic Riccati equation," *IEEE Trans. Autom. Control*, vol. 35, no. 3, pp. 348–350, Mar. 1990.

Changick Song (S'09–M'13) received the B.S., M.S., and Ph.D. degrees in electrical engineering from Korea University, Seoul, South Korea, in 2007, 2009, and 2012.

He was a Visiting Researcher with the University of Southern California, Los Angeles, CA, USA in 2009, and at Queens University, Kingston, ON, Canada, in 2011. From September 2012 to April 2013, he was a Research Professor with Korea University, and from May 2013 to August 2014, he was with the Communications and Signal Processing (CSP) Group, Imperial College, London, U.K., as a Postdoctoral Research Associate. In September 2014, he joined the faculty of Korea National University of Transportation, Chungju, South Korea, where he is currently an Associate Professor with the Department of Electronic Engineering. His research interest includes information theory and signal processing for wireless communications and security.

Hoon Lee (S'14–M'18) received the B.S. and Ph.D. degrees in electrical engineering from Korea University, Seoul, South Korea, in 2012 and 2017.

In 2015, he visited Imperial College London, London, U.K., to conduct a collaborative research. In 2017, he was a Post-Doctoral Fellow with Korea University. In 2018, he joined the Singapore University of Technology and Design, Singapore, where he is currently a Post-Doctoral Fellow. His research interests include machine learning and signal processing for wireless communications such as visible light communications, wireless energy transfer communication systems, and secure wireless networks.

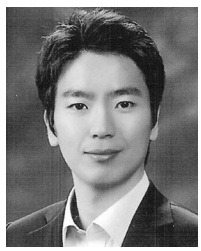

Kyoung-Jae Lee (S'06–M'11) received the B.S. and Ph.D. degrees in electrical engineering from Korea University, Seoul, South Korea, in 2005 and 2011, respectively.

He was an Intern with Beceem Communications, Inc., Santa Clara, CA, USA, in 2007, and he was a Visiting Student with the University of Southern California, Los Angeles, CA, USA, in 2009. He was a Research Professor with Korea University, in 2011. From 2011 to 2012, he was a Postdoctoral Fellow with the Wireless Networking and Communications Group, The University of Texas at Austin, Austin, TX, USA. Since 2012, he has been with Hanbat National University, Daejeon, South Korea, where he is currently an Associate Professor with the Department of Electronics and Control Engineering. His research interests include communication theory, signal processing, and information theory applied to the next-generation wireless communications.

Dr. Lee was the recipient of Best Paper Award at the IEEE VTC Fall in 2009, the IEEE ComSoc APB Outstanding Paper Award in 2013, and the IEEE ComSoc APB Outstanding Young Researcher Award in 2013.